Cold-water coral mounds in the western Mediterranean Sea: New insights into their initiation and development since the Mid-Pleistocene in response to changes of African hydroclimate

C. Wienberg [a, *], T. Krengel [b], N. Frank [b], H. Wang [a, c], D. Van Rooij [d], D. Hebbeln [a]

[a] MARUM - Center for Marine Environmental Sciences, University of Bremen, Leobener Strasse 8, 28359, Bremen, Germany
[b] Institute of Environmental Physics (IUP), Heidelberg University, Im Neuenheimer Feld 229, 69120, Heidelberg, Germany
[c] State Key Laboratory of Marine Geology, Tongji University, Siping Road 1239, 200,092, Shanghai, China
[d] Renard Centre of Marine Geology, Department of Geology, Ghent University, Krijgslaan 281 S8, B-9000, Gent, Belgium

ARTICLE INFO

ABSTRACT

This study presents sediment cores up to 70 m long collected by the sea floor drill rig MARUM-MeBo70 from cold-water coral mounds in the western Mediterranean Sea. From these cores, an unprecedented data set of 200 Th/U coral ages has been obtained, greatly expanding our knowledge of the evolution of Mediterranean coral mounds. The drill records provided new insights into the initiation of the Mediterranean coral mounds as the base of a 60-m-high mound was penetrated and dated to the Mid-Pleistocene (~390 ka). We also found that mound initiation was non-synchronous as larger mounds possibly initiated already during the Mid-Pleistocene Transition. During the last 480 kyr, mound development occurred in short and intense pulses (duration: ~10−30 kyr; aggradation rates: 20−275 cm kyr^{-1}), which could not be assigned to ice age-paced oscillations, but showed a remarkably coherent pattern with precession-driven changes in African hydroclimate. Increased dust supply, related to a desertification of the Sahara and northern Africa, appears to have boosted mound development by enhancing productivity conditions (to promote coral growth) and sediment supply (to promote mound aggradation). In addition, mound development is closely linked to the well-ventilated and nutrient-rich Levantine Intermediate Water and internal wave activity associated to this water mass that provided turbulent conditions and enhanced the lateral delivery of food and sediments. During African humid periods, increased freshwater input into the Mediterranean impaired the formation of Levantine Intermediate Water, which most likely resulted in low-energy and oxygen-depleted living conditions for Mediterranean coral communities. This study shows the importance to consider past changes in continental hydroclimate and their implications on oceanic processes to fully understand the complex environmental controls on coral mound development. In the Mediterranean Sea, such land-atmosphere-ocean feedback processes are especially amplified due to its latitudinal placement between two climate regimes, making this basin and its deep-sea ecosystems most vulnerable to past and future climate change.

1. Introduction

The Mediterranean Sea offers appropriate environmental conditions for cold-water corals (CWCs) in many areas. Especially in its western and central basins, abundant living and fossil CWC communities have been documented from submarine canyons along the northern Mediterranean margin, from escarpments flanking plateaus, banks and troughs, and from seamounts and mud volcanoes (e.g., Freiwald et al. 2009; Orejas et al., 2009; Margreth et al., 2011; Würtz and Rovere, 2015; Taviani et al., 2016; Taviani et al., 2017; Chimienti et al., 2019; Rüggeberg and Foubert, 2019; Vertino et al., 2019; Gori et al. accepted). In recent years, also a growing number of coral mound provinces (CMPs) - constructed by the scleractinian CWCs *Desmophyllum pertusum* (recently

---

* Corresponding author.
E-mail addresses: cwberg@marum.de (C. Wienberg), Thomas.Krengel@iup.uni-heidelberg.de (T. Krengel), Norbert.Frank@iup.uni-heidelberg.de (N. Frank), hwang147@tongji.edu.cn (H. Wang), David.VanRooij@UGent.be (D. Van Rooij), dhebbeln@marum.de (D. Hebbeln).

reassigned from the genus *Lophelia*; Addamo et al., 2016) and *Madrepora oculata* - has been discovered (Fig. 1a), such as on the Apulian margin in the Ionian Sea (e.g., Freiwald et al. 2009; Vertino et al., 2010; Fink et al., 2012; Savini et al., 2014), in the Strait of Sicily (Martorelli et al., 2011), on the Tunisian margin and in the Corsica Channel in the Tyrrhenian Sea (Angeletti et al., 2020; Corbera et al., 2022), and on the Spanish margin in the northern Alborán Sea (Lo Iacono et al., 2019; Sánchez-Guillamón et al., 2022). The Moroccan margin in the southern Alborán Sea, however, exhibits a hotspot region for coral mound development, represented by three extended CMPs (referred to as the East Melilla, West Melilla, and Cabliers CMPs; Fig. 1b) comprising numerous coral mounds at water depths of ~210−700 m with some mounds rising up to 140−150 m above the seafloor (Lo Iacono et al., 2014; Corbera et al., 2019; Hebbeln, 2019).

The development of coral mounds primarily depends on sustained coral growth. Following their initiation, triggered by the settlement of coral larvae on any type of hard substrate (e.g., Wheeler et al., 2011), coral mounds undergo cyclic stages of development comprising periods of (i) prolific CWC growth forming large reef structures that promote mound growth, (ii) CWC decline leading to a significant slow-down or stagnation in vertical mound aggradation, and (iii) repopulation of CWC that initiates the next stage of mound development (e.g., Roberts et al., 2006). Coral mounds evolve over geological timescales (1.000s−100.000s of years) and are therefore valuable sedimentary archives that document recurring phases of flourishing CWC reefs controlled by environmental changes (e.g., Kano et al., 2007; Frank et al., 2011; Wienberg and Titschack, 2017; Lo Iacono et al., 2018). However, coral mound development is not just the result of sustained coral growth, they additionally rely on the concurrent supply and deposition of terrigenous sediments under energetic hydrodynamic conditions (e.g., Roberts et al., 2006; Titschack et al., 2009; Wienberg and Titschack, 2017). Dense frameworks of living CWCs have the capability to locally modulate sedimentary and hydrodynamic processes on the mound as they provide a low-energy environment, which allows suspended bypassing sediments to become deposited in between the coral branches (known as baffling effect), and prevents the remobilisation of these fine-grained sediments (e.g., Huvenne et al., 2009; Hennige et al., 2021). The entrapped sediments stabilize the reef framework, prevent its collapse, and thus, support vertical mound growth (e.g., Titschack et al., 2016; Wang et al., 2021). Moreover, model simulations showed that also the mounds themselves influence the hydrodynamics around them (Cyr et al., 2016; Mohn et al., 2014; van der Kaaden et al., 2021). With increasing mound height, tide-topography interactions may lead to an increase in vertical velocities. This results in energy being highest on the top and upper flanks of the mound, which promotes CWC growth by providing a stable mechanism for food supply, which in turn has a positive
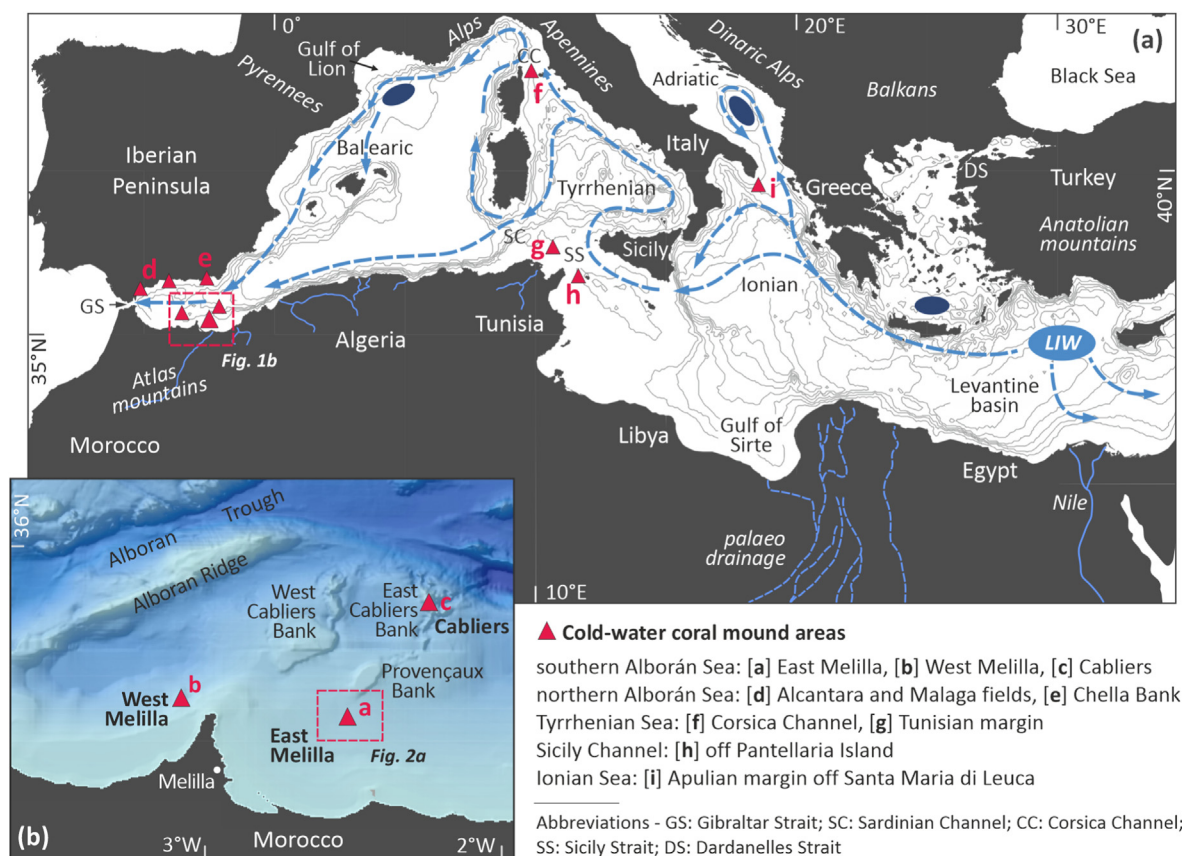

Fig. 1. Study area. (**a**) Bathymetric overview map of the Mediterranean Sea showing its complex topography with several deep basins connected by shallow straits. The blue bold dashed line indicates the flow pathway of the Levantine Intermediate Water (LIW; modified after Millot and Taupier-Letage 2005; Hayes et al. 2019), which is formed in the Levantine basin (light blue oval). The LIW spreads throughout the entire Mediterranean Sea and conditions deep-water formation in the northern Mediterranean areas (dark blue ovals). Also shown are the Nile river draining into the Levantine basin, a palaeo-river system flowing northward from the Saharan watershed into the Gulf of Sirte, which was activated during strong African monsoon (Osborne et al. 2010; Blanchet et al. 2021; Ehrmann and Schmiedl 2021), numerous smaller rivers draining from the Atlas Mountains into the western Mediterranean basin (blue lines), and high mountains surrounding the Mediterranean basin. (**b**) Shaded-relief map of the southern Alborán Sea showing the East and West Melilla and the Cabliers coral mound provinces. Red triangles on both maps indicate coral mound areas (a to h; for references see text). (For interpretation of the references to colour in this figure legend, the reader is referred to the Web version of this article.)

feedback on vertical mound growth (van der Kaaden et al., 2021). Therefore, to decipher the development of coral mounds in the past, we need a comprehensive knowledge of the interplay of biological, sedimentological, and hydrographic processes and their variations through time in response to climate change.

In the Mediterranean Sea, the study of coral mound development in relation to paleoceanographic variations during the Pleistocene and Holocene is mainly concentrated on the CMPs in the southern Alborán Sea. Sediment cores obtained from these CMPs, all recorded a highly prolific period for CWCs starting during the last deglaciation (~14−15 ka) and lasting until the end of the Early Holocene (~8−9 ka), which resulted in mound development with remarkably high vertical mound aggradation rates (ARs) of ~100−400 cm kyr^{-1} (Fink et al., 2013; Stalder et al. 2015, 2018; Wang et al., 2019; Fentimen et al., 2020; Corbera et al., 2021; Korpanty et al. submitted). This thriving phase has been ascribed to regional environmental conditions of enhanced (surface and export) productivity and moderate to strong hydrodynamics maintaining coral growth and sediment supply (Fink et al., 2013; Stalder et al., 2015; Fentimen et al., 2020; Portilho-Ramos et al., 2022). Such conditions were most likely further supported by the activity of internal waves, which enhanced turbulence and increased the delivery of food and sediment particles at the interface between the Levantine Intermediate Water (LIW) and overlying Atlantic water (Wang et al., 2019; Corbera et al., 2021).

The Mid-to Late Holocene mound development displayed a contrasting pattern. For both Melilla CMPs, mound development significantly reduced during the Holocene (Fink et al., 2013; Wang et al., 2019; Wienberg, 2019), while exceptionally thriving CWCs are found on some northern mounds of the Cabliers CMP until today (Corbera et al., 2021). Hence, the present-day reef status prevailing at the respective CMPs varies in close vicinity of 50−60 km from extinct reefs, to scattered and small live coral colonies and to thriving reefs (Hebbeln et al., 2009; Lo Iacono et al., 2014; Corbera et al., 2019). These differences in the present-day coral vitality are likely conditioned by locally acting processes, which still need to be fully identified.

Because the coral records available to date from the Mediterranean Sea are based only on dredged surface corals (e.g., McCulloch et al., 2010) and sediment cores no longer than 10 m (e.g., Corbera et al., 2021), our knowledge of the timing of CWC occurrence prior to the last deglaciation and of the initiation and evolution of coral mounds over several climate oscillations is still very limited. CWCs were present in the Mediterranean Sea since ~480 ka (proved by a single dated surface coral sample from the Strait of Sicily; McCulloch et al., 2010), and possibly already since the Early Miocene as documented from rock outcrops in Italy (~20 - 16 Ma; Vertino et al., 2019). A core record recently recovered from a coral mound of the Cabliers CMP in the southern Alborán Sea documented periodic coral growth since ~370 ka corresponding to warm and cold climate periods, though mound development was apparently hampered during glacial periods as indicated by very low ARs of <5 cm kyr^{-1} (Corbera et al., 2021). Another recent study of coral mounds on the Tunisian continental margin (Tyrrhenian Sea) has shown that CWCs were present in this central region of the Mediterranean Sea since ~390 kyr, but that mound development was restricted during most of this period (Corbera et al., 2022). However, one stage of (moderate) mound development occurred during the last glacial period (~15−33 ka with ARs of up to ~20 cm kyr^{-1}; Corbera et al., 2022), which contrasts to the findings in the southern Alborán Sea (Fink et al., 2013; Wang et al., 2019; Corbera et al., 2021).

These few CWC documentations hint already to their sensitivity to climate-forced environmental changes, which were especially amplified in the Mediterranean due to the small size of the semi-enclosed basin and its latitudinal position between two climate regimes (Lionello et al., 2006). For instance, changes in (i) ocean thermohaline circulation as well as productivity both regulating the supply of food; (ii) oxygen and thermal conditions of ambient water masses that affect the physiological processes of corals; (iii) freshwater discharge as well as fluvial and aeolian sediment input, controlled by African continental climate change; and possibly also (iv) the effect of a lowered sea level on basin size and continental shelf geometry certainly had a profound impact on the Mediterranean coral communities (e.g., Remia and Taviani, 2005; McCulloch et al., 2010; Frank et al., 2011; Fink et al., 2012; Naumann et al., 2014; Stalder et al., 2018; Vertino and Corselli, 2019). However, our understanding of the triggering environmental factors that led to the bloom or decline of CWCs, and hence, to the development of coral mounds in the Mediterranean basin is still far from being complete.

To overcome this limitation, up to 70-m-long sediment cores were collected by the sea floor drill rig MARUM-MeBo70 from two ridge-shaped coral mounds of the East Melilla CMP during R/V Maria S. Merian expedition MSM36 ("MoccoMeBo"; Hebbeln et al., 2015). These long sedimentary records are unique, as for the first time a 60-m-high coral mound in the western Mediterranean Sea was penetrated down to its base. Based on an unprecedented data set of 200 Th/U coral dating obtained from the two MeBo cores and additional gravity cores, this study (i) determines the timing of coral mound initiation in the southern Alborán Sea, and (ii) contributes to our knowledge on coral mound development in the western Mediterranean since the Mid-Pleistocene under the influence of climate-induced environmental changes.

2. Regional setting

The Mediterranean Sea is a marginal sea, which is characterised by several peculiarities. It has a land-locked nature and is surrounded by high mountain chains (South Europe: Pyrenees, Alps, Apennines, Dinaric Alps, Balkans; Asia: Anatolian Mountains; North Africa: Atlas Mountains; Fig. 1a; Lionello et al., 2006), which influence the local to regional wind flow and precipitation pattern (Smith, 1979; Sandu et al., 2019). It is a semi-enclosed basin, being connected to the Atlantic Ocean only through the narrow Strait of Gibraltar (sill depth: ~300 m). Its water budget is regulated by the net inflow of Atlantic water, the inflow from the Black Sea at the Dardanelles Strait, evaporation, precipitation, and river discharge. Evaporation largely dominates the Mediterranean water budget, and the resulting freshwater deficit is only balanced during spring by freshwater input from river discharge and precipitation (e.g., Struglia et al., 2004). The topography of the Mediterranean Sea is characterised by deep basins (east: Levantine Basin and Ionian Sea; west: Tyrrhenian, Balearic, and Alborán Seas), connected by rather shallow straits (Strait of Sicily, Sardinian and Corsica Channels; Fig. 1a), which have a strong impact on the circulation pattern (e.g., Schroeder et al., 2012).

The Mediterranean Sea represents a kind of "*miniature ocean*" due to the strong formation of intermediate and deep waters facilitating a Mediterranean thermohaline circulation, though these processes occur on a much shorter turnover timescale compared to the global oceans (Bethoux et al., 1999; Schroeder et al., 2012). The LIW is the most voluminous water mass produced in the Mediterranean, and hence, the main driver for the Mediterranean thermohaline mixing and overturning circulation (Skliris, 2014). This warm and saline water mass is formed in the Levantine basin in the eastern Mediterranean Sea (Fig. 1a) driven by an excessive evaporation of the surface layer in combination with a freshwater input deficit (Pinardi and Masetti, 2000; Schroeder et al., 2012). It spreads throughout the entire Mediterranean basin, crosses the Strait of

Sicily (sill depth: ~500 m), which acts as a key choke point separating the sea in two main basins (Fig. 1a), and carries large volumes of high-saline water from the eastern to the western basin (e.g., Schroeder et al., 2017). The LIW circulates along-slope at intermediate depths of ~200−600 m, reaching velocities of up to 14 cm s^{-1} along the slope of the Alborán Sea (Millot, 1999; Millot and Taupier-Letage, 2005; Schroeder et al., 2012; Ercilla et al., 2016; Hayes et al., 2019). The amount of heat and salt carried by the LIW varies over different time scales (interannual to decadal) and has a strong impact on the deep-water formation in the western Mediterranean as it can enhance or depress deep convection (e.g., Margirier et al., 2020; Amitai et al., 2021).

The Western Mediterranean Deep Water (WMDW) is formed in the Gulf of Lion (Millot, 1999) and mixes with the LIW, both flowing through the Strait of Gibraltar forming the Mediterranean Outflow Water. Surficial less-saline Atlantic water entering through the Strait of Gibraltar flows eastwards into the basin at maximum water depths of 150−200 m with current velocities of up to 1 m s^{-1} (Parrilla et al., 1986). It enters the Alborán Sea in pulses and regulates in conjunction with the LIW the intensity of the thermohaline circulation. The Atlantic water describes two large anticyclonic gyres, which control the surface circulation in the Alborán Sea and locally increase surface productivity (Heburn and La Violette, 1990).

2.1. The link between Levantine Intermediate Water and Mediterranean cold-water corals

Living Mediterranean CWCs are today usually found at depths bathed by the LIW revealing their link to the flow pathway of this well-ventilated and nutrient-rich intermediate water mass (e.g., Taviani et al., 2017; Chimienti et al., 2019; Corbera et al., 2019; Vertino et al., 2019). Yet, it is likely not the water mass itself that fosters coral proliferation. The interface or transition between the high-saline LIW and the overlying low-saline Atlantic water is characterised by steep vertical and horizontal density gradients (Millot, 1999). Such pycnoclines become disturbed when they intersect a sloping topography (shelf edge, continental slope, seamount, tectonic ridge) resulting in the formation of high-energetic internal waves (Puig et al., 2004; Ercilla et al., 2016). Internal waves generate currents causing enough turbulence to erode, resuspend and laterally distribute bottom sediments, and are thought to have controlled the development of contourites (drifts and terraces) that formed throughout the Alborán Sea during the Pliocene and Quaternary (Ercilla et al., 2016; Juan et al., 2016). It is well-known that internal waves also have the potential to affect the distribution and prosperity of CWC reefs as they are fundamental mechanisms to increase vertical mixing and lateral supply influencing the distribution of nutrients, particulate organic material, plankton and larvae, and to induce large variations in temperature and oxygen (e.g., Frederiksen et al., 1992; Mienis et al., 2007; Davies et al., 2009; White and Dorschel, 2010; Hanz et al., 2019). For the northern and central Alborán Sea, internal waves with amplitudes of 90−150 m are reported from the pycnocline between the LIW and Atlantic water at ~250 m water depth and at a (weaker) vertical density gradient within the LIW layer at ~500 m depth (van Haren, 2014). Internal waves are also known to act off Morocco from the shelf edge at 100−150 m down to 400 m depth (Ercilla et al., 2016).

2.2. The East Melilla coral mound province in the southern Alborán Sea

The East Melilla CMP in the southern Alborán Sea (western Mediterranean) was first mentioned by Comas and Pinheiro (2007), and was re-visited during several following expeditions (e.g.,

Comas et al., 2009; Hebbeln et al., 2009; Hebbeln et al., 2015; Van Rooij et al. 2017). It is framed (i) by the West Melilla CMP to the west (Fig. 1b), comprising conical-shaped and mainly small (<10 m in height above the seafloor) coral mounds, which developed in 300−430 m water depth on the southern flank and at the base of a volcanic outcrop (Lo Iacono et al., 2014); and (ii) by the Cabliers CMP to the north (Fig. 1b), where ridge-shaped mounds with average heights of ~80 m developed in 250−710 m depth on top of a volcanic basement (East Cabliers Bank; Corbera et al., 2019). The East Melilla CMP is located below the shelf edge on the upper Moroccan slope in water depths of 210−475 m and comprises mounds grouped into three slope-parallel E-W-trending belts (Hebbeln, 2019). The shallow southernmost belt comprises several sinuous to elongated coral ridges at ~210−240 m water depth (e.g., Dragon and Elf mounds; Fig. 2a). The ridges stretch over several kilometres in a NW-SE direction and are partly buried by sediments. They rise on average 10−20 m above the surrounding seafloor, but also extend several tens of metres below the seafloor (Fig. 2b; Hebbeln et al., 2015).

Directly north of the southern belt, oval-shaped to elongated coral mounds form a central belt in water depths of ~240−320 m (e.g., Mole, Horse and Serpent mounds; Fig. 2a). These mounds display steep flanks and have average heights of 20−40 m above the seafloor (Hebbeln, 2019). Towards the north follows a 9-km-wide area barren of any mound structures. The northern belt comprises only three but impressively large coral ridges (Brittlestar ridges (BRs) I to III; Hebbeln et al., 2009). The BRs have steep flanks, stretch between 3 and 20 km in length and rise 50−150 m from above the surrounding sea floor in ~375−475 m water depth (Hebbeln, 2019). They are attached to the southern flank of the Provençaux Bank (Fig. 2a), a volcanic structure with a flat and shallow summit that rises to a water depth of ~200 m (Ammar et al., 2007). The zig-zag-like orientation of the BRs (Fig. 2a) follows main regional fault directions (Martínez-García et al., 2011). Thus, tectonics may have played an important role as a pre-conditioning factor for their initiation, although there is still no information on the actual nature of the basement of these ridges (Comas and Pinheiro, 2007; Hebbeln, 2019). However, strong bottom currents had likely a much more important influence on the overall development of the East Melilla coral mounds indicated by well-developed moats lined with contourites surrounding the mounds (Fig. 2; Comas et al., 2009; Hebbeln et al., 2016; Hebbeln, 2019).

3. Material and methods

3.1. Core material collected with the sea floor drill rig MeBo70 and gravity corer

The sea-floor drill rig MARUM-MeBo70 (MARUM, University of Bremen, Germany) is a mobile drilling system that is deployed on the sea floor and operates remotely from a research vessel (Freudenthal and Wefer, 2013). During expedition MSM36 ("MoccoMeBo") in 2014, the MARUM-MeBo70 was deployed from the R/V Maria S. Merian to obtain long sediment cores from coral mounds of the East Melilla CMP (Hebbeln et al., 2015). One MeBo core was retrieved from the 140-m-high BRI (GeoB18118-2) and one from the much shallower and smaller ridge-shaped Dragon mound, which rises 20−30 m above the sea floor (GeoB18116-2; Fig. 2a−c). For both drilling sites, a maximum coring depth of ~71 m below the sea floor was reached with high sediment recoveries of 73% (equivalent to ~53 m of sediment) for BRI and of 96% (equivalent to ~70 m of sediment) for Dragon mound (Table 1; see also Supplementary material). The MeBo core from BRI showed throughout coral fragments embedded in a hemipelagic sediment matrix. A recent study of a gravity core, collected in close proximity to the
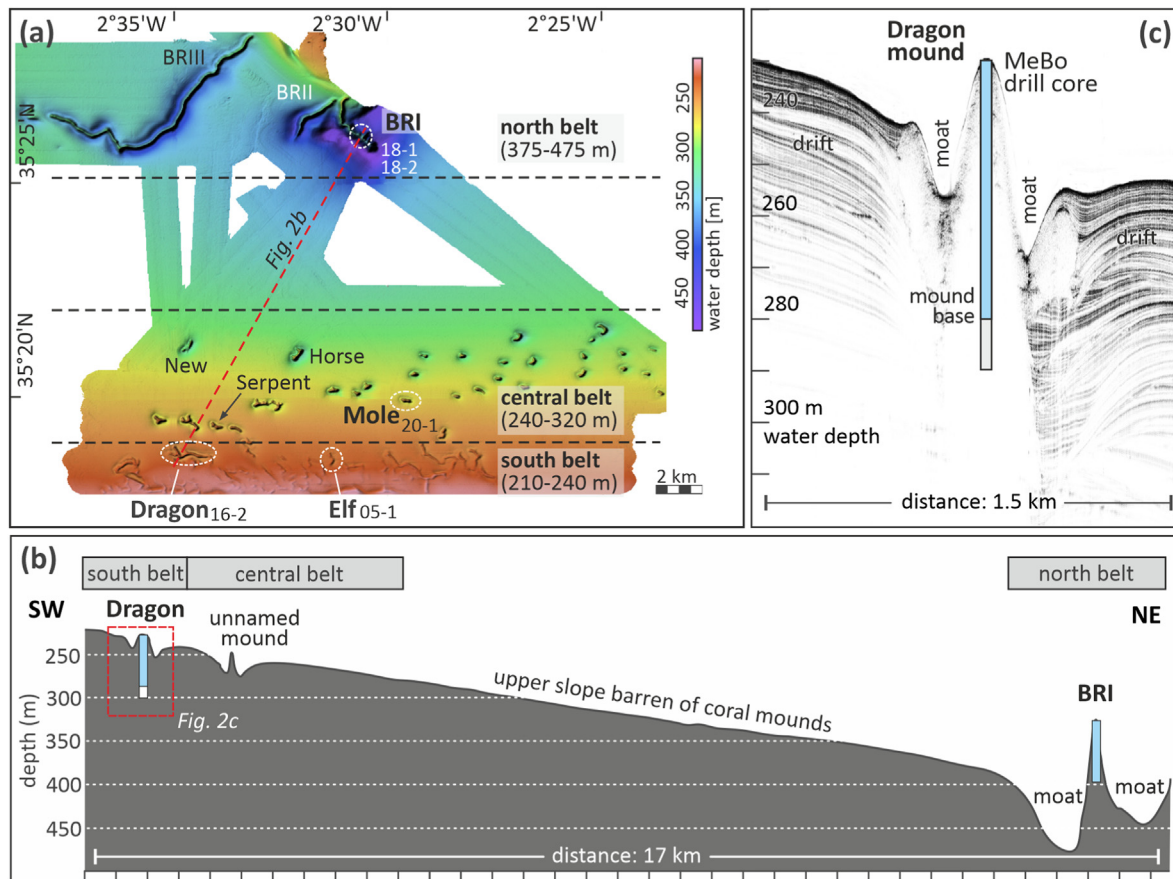
Fig. 2. The East Melilla cold-water coral mound province. (**a**) Shaded-relief map showing the East Melilla coral mounds/ridges, which are grouped into three belts (modified after Hebbeln 2019). The location of MeBo drill sites on top of Brittlestar ridge I (BRI) and Dragon mound, and gravity cores collected from BRI, Mole and Elf mounds are indicated by dotted circles (core-IDs: GeoB181xx-x). The dashed red line indicates the position of the altitude profile shown in Fig. 2b. (**b**) Altitude profile crossing the MeBo drill sites on top of the shallow Dragon mound in the SW and of the steep and large BRI in the NE. The dashed red box indicates the drill site on Dragon mound shown in detail in Fig. 2c. (**c**) Sub-bottom profile showing the Dragon mound surrounded by moats and drift sediments. The position of the MeBo core penetrating the mound base is indicated (blue: coral-bearing sediments, white: coral-barren sediments). (For interpretation of the references to colour in this figure legend, the reader is referred to the Web version of this article.)

Table 1
Metadata of MeBo drill cores and gravity cores collected from the East Melilla coral mound province during R/V Maria S. Merian expedition MSM36 ("MoccoMeBo"). DRD: maximum drill depth; No. Co: Number of core barrels (each MeBo core consisted of 30 core barrels à 2.35 m length); No. Th/U: Number of obtained Th/U ages; BRI: Brittlestar ridge I; GC: gravity core.

Coral mound	Core ID	Gear	Latitude	Longitude	Water depth	DRD (mbsf)	Recovery	No. Co	No. Th/U
Dragon	GeoB18116-2	MeBo	35°18.642′N	2°34.933′W	236 m	70.85	70 m (96%)	30	76
BRI	GeoB18118-2	MeBo	35°26.139′N	2°30.765′W	332 m	70.85	53 m (73%)	30	45
Elf	GeoB18105-1	GC	35°18.440′N	2°31.318′W	224 m	/	5.7 m	1	10
Mole	GeoB18120-1	GC	35°19.883′N	2°29.603′W	249 m	/	10.1 m	1	15
BRI	GeoB18118-1[a]	GC	35°26.139′N	2°30.765′W	332 m	/	8.7 m	1	54

[a] Gravity core GeoB18118-1 was retrieved at the same position as the MeBo core GeoB18118−2 as a supplement for the upper part of the drill core collected at BRI.

MeBo drilling site at the BRI, showed that the matrix sediments are dominated by fine (medium silt) siliciclastic sediments (Wang et al., 2021). The MeBo core from Dragon mound contained coral fragments only in the upper 60 m, while below this depth, the core was exclusively composed of hemipelagic sediments without any coral fragments (Fig. 2c). Both MeBo cores showed no signs of lithification (neither minor induration nor cementation) in the downcore record, which otherwise would be an indicator for diagenetic physicochemical processes (e.g., van der Land et al., 2014). In addition, during an extensive ROV video reconnaissance over the central sector of the BRI, crossing its summit (including the MeBo

drill site) and adjacent flanks, no exposed lithified sediments (hardgrounds) were observed (Hebbeln et al., 2009). The two long MeBo coral records were supplemented by three gravity cores, which were collected from each of the three mound belts (Table 1; Fig. 2a) allowing to study any potential inter-mound variability in mound development. All gravity cores were entirely composed of coral fragments embedded in hemipelagic sediments. As it has been suggested that steep slopes of coral mounds in particular might be affected by mass-wasting (e.g., Eisele et al., 2014), all MeBo and gravity cores were taken from the summits of the East Melilla mounds to minimize the risk that the sedimentary records

contain units of significantly reworked/redeposited coral material.

3.2. Th/U dating

Well-preserved fragments of the framework-forming species *D. pertusum* and *M. oculata* were sampled at various core depths from all MeBo and gravity cores. The coral fragments were Th/U dated according to the procedures described in detail by Wefing et al. (2017) and using the new ^{230}Th and ^{234}U half-life values published in Cheng et al. (2013). Prior to the measurements, all coral fragments were cleaned mechanically and chemically according to a procedure described by Frank et al. (2004). Sample preparation, chemical purification of the Th and U fractions, and mass spectrometric analyses were carried out at the Institute for Environmental Physics (IUP, University of Heidelberg, Germany) using a multi-collector inductivity coupled plasma mass spectrometer (ThermoFisher Neptune plus). Absolute Th/U dates (reported as kiloyear, ka; Table S1 of the Supplementary material) were considered reliable and used for further discussion, when measured ^{232}Th concentrations were <10 ppb and the initial δ^{234}U$_i$ values ranged between $\pm$10‰ compared to the value of modern Mediterranean seawater (149.0‰; according to Border (2020) Mediterranean water masses are elevated by ~1–2‰ in δ^{234}U compared to the Atlantic; see Fig. S2 of the Supplementary material).

3.3. Interpretation of coral age clusters, hiatuses and mound aggradation rates (ARs)

Sediment cores obtained from coral mounds often exhibit discontinuous stratigraphic records. They typically display distinct age clusters consisting of stratigraphically closely related coral ages, which indicate periods of sustained coral growth (e.g., López-Correa et al., 2012; Douarin et al., 2013; Matos et al., 2015; Wienberg et al., 2018; Raddatz et al., 2020; 2022). Such age clusters are either separated by thin core sequences with small numbers of coral ages, or by distinct hiatuses, i.e. temporal gaps in the stratigraphic record. While core intervals with few coral ages reflect a temporary sparse occurrence of CWCs, hiatuses are primarily interpreted as periods without coral growth (e.g., Frank et al., 2009; Douarin et al., 2013; Bonneau et al., 2018; Wienberg et al., 2018; Corbera et al., 2021). Few early coral mound studies also suggested erosion (i.e. mass wasting) as a possible cause of hiatuses, but without providing clear evidence for this scenario (Dorschel et al., 2005; Eisele et al., 2008). Nevertheless, mass wasting may have the potential to affect the "*coral record*" by causing random patterns of erosion and preservation in the individual records. However, no clear evidence of mass wasting has yet been found for the coral mounds in the southern Alborán Sea, while there are several indications that temporary interruptions in coral growth were in most cases the more probable explanation for the stratigraphic gaps in the "*coral record*" (see discussion below).

Coral ages are used to calculate vertical mound ARs. Because coral ages within a cluster do not always follow a strict chronological order, but may also reveal age reversals or display ages with a scattered distribution (e.g., resulting from the collapse of coral colonies/frameworks or break-off of larger coral branches; see Titschack et al., 2016), an age-to-age calculation of ARs is often not possible (see for example Wienberg et al., 2018). For this study, the oldest and youngest coral ages of an age cluster in relation to the maximum and minimum core depths of the respective core interval (bordered by hiatuses) were used for the calculation of ARs (reported in cm kyr^{-1}; Table S1 of the Supplementary material) providing rather conservative estimations. This method was also applied to re-calculate previously published ARs (Corbera et al.,

2021) used for discussion.

Mound development associated with high mound ARs, which can exceed sedimentation rates in adjacent sedimentary environments of about an order of magnitude (see e.g., Titschack et al., 2015; Wang et al., 2021), is indispensably linked to times of sustained coral growth. According to Frank et al. (2009), we define ARs of >15 cm kyr^{-1} as representative of densely populated coral mounds leading to enhanced mound development, while ARs of <15 kyr^{-1} down to zero are interpreted as times of reduced or stagnated mound development. During times without coral growth (or a very limited occurrence of CWCs), coral mounds remain in an "*inactive*" or "*dormant*" state (according to Wienberg and Titschack, 2017). Without the presence of a dense living reef framework and its capability to baffle bypassing suspended sediments even under turbulent conditions (e.g., Huvenne et al., 2009; Hennige et al., 2021; Wang et al., 2021), on-mound sedimentation of hemipelagic sediments is primarily controlled by regional changes in bottom current strength that steer deposition during weak bottom current conditions, and non-deposition or erosion (i.e., winnowing) during strong bottom current conditions, in any case resulting in very low to zero (net) ARs. Moreover, neither non-deposition nor erosion of fine sediments would impair the completeness of the coral record, which is in the focus of this study.

4. Results

In total, 200 Th/U coral ages were obtained from the MeBo and gravity cores collected from coral mounds of the East Melilla CMP, which altogether encompass ~480 kyr (Table S1 of the Supplementary material). All core records revealed distinct age clusters, which are separated by core intervals with a low number of coral ages, or by one or more hiatuses (Fig. 3). In the following, the coral age distribution patterns are described for each core separately. The observed patterns are temporally related to the benthic oxygen isotope stack of Lisiecki and Raymo (2005) with Marine Isotope Stages (MIS) with even numbers representing glacial periods and odd numbers corresponding to warm climate periods (i.e. interglacial complexes containing a number of temperate intervals within them; excluding MIS 3 which is not considered as an interglacial). To avoid confusion, please note that we used the substage nomenclature recently recommended by Railsback et al. (2015), and we considered the substages MIS 11a, MIS 9e, MIS 7e, MIS 7a-c and MIS 5e as full interglacials according to the Past Interglacials Working Group of PAGES (2016), while other substages of interglacial complexes are referred to as stadials and interstadials.

The **MeBo core GeoB18116−2** was collected from the western top of the E-W elongated **Dragon mound** (236 m depth), which is part of the most southern and shallowest coral mound belt in the East Melilla CMP (Fig. 2a). The base of Dragon mound lies ~60 m below the seafloor (Fig. 2c) and the oldest dated coral fragment corresponding to this depth, and marking its initiation time, showed an age of ~390 ka (Fig. 3). Overall, all coral ages (n = 76) obtained from Dragon mound ranged from 390.5 ± 10.4 to 102.6 ± 0.5 ka (Table S1 of the Supplementary material). From 60 to ~27 m core depth, the Th/U ages ranged from 391 to 297 ka (MIS 11a to MIS 9b) and were largely ordered non-chronologically. The majority of ages corresponded to the glacial period of the MIS 10 and to the MIS 9b-d (Fig. 3). Due to the large scatter of the ages, we should interpret any AR calculation with caution; however, during MIS 10 and MIS 9d-b ARs were clearly enhanced (~50–60 cm kyr^{-1}), while ARs were significantly lower (~5–8 cm kyr^{-1}) during MIS 11a and the full interglacial of MIS 9e. During the following ~60 kyr, covering the MIS 9a, the entire glacial period of MIS 8, and the full interglacial MIS 7e, only three coral
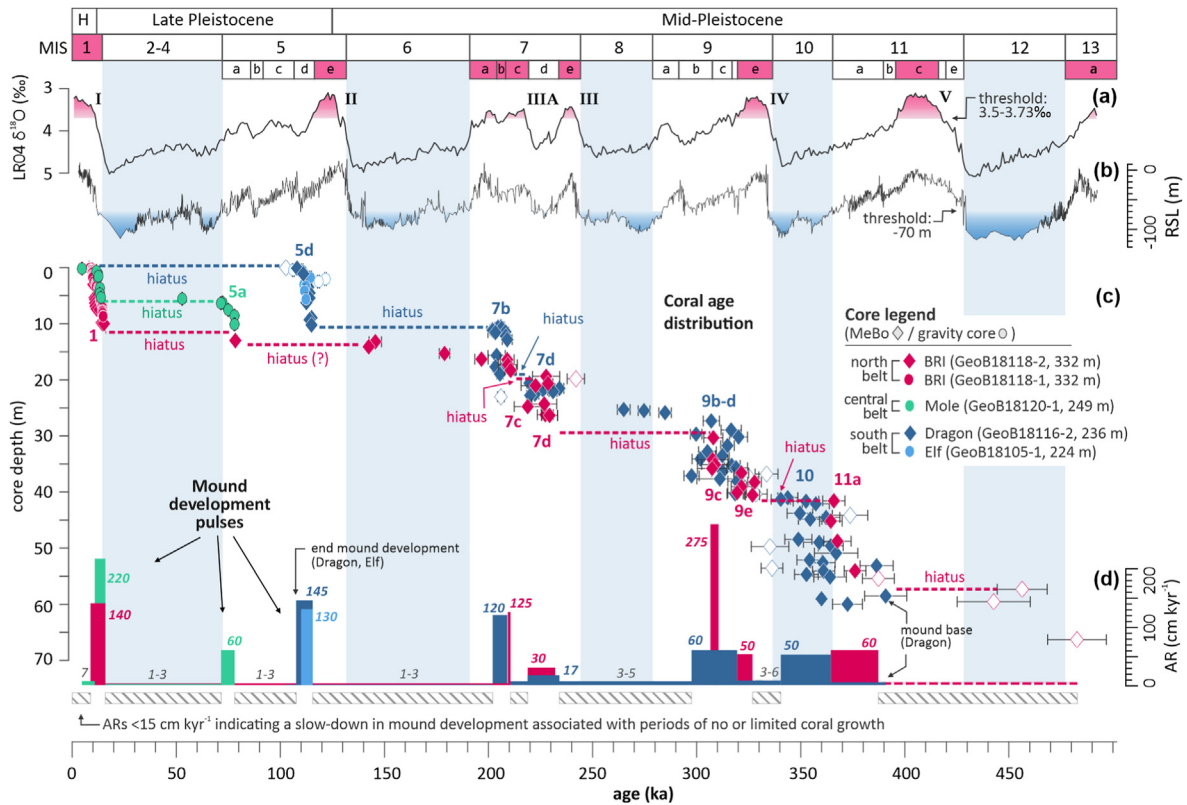
Fig. 3. Coral age distribution and mound aggradation rates. (**a**) LR04 Global Pleistocene benthic δ¹⁸O stack (Lisiecki and Raymo 2005); terminations I to V are indicated. Boundaries between Marine Isotopes Stages (MIS) and sub-stage intervals according to Railsback et al. (2015), the full interglacials MIS 1, 5e, 7a-c, 7e, 9e, 11c and 13a are indicated (pink filling of LR04 stack with a threshold at 3.5-3.73‰; according to the Past Interglacials Working Group of PAGES, 2016). Light blue vertical bars indicate glacial periods. H: Holocene. (**b**) Sea-level curve (blue filling with a threshold at -70 m; Grant et al. 2014). (**c**) Coral ages (versus core depth) obtained from two long MeBo drill cores (diamond symbols; maximum drill depth: 70 m) and three gravity cores (dot symbols; core recoveries: 5.7 - 10.6 m; see legend for colour code, mound name, core ID and water depth). The coral-bearing cores were collected from coral mounds of the northern (Brittlestar ridge I, BRI), central (Mole mound) and southern belts (Dragon and Elf mounds) of the East Melilla coral mound province (see Fig. 2a for core locations). (**d**) Calculated mound aggradation rates (ARs, numbers next to the bars given in cm kyr⁻¹; bars follow the same colour code as in c). High ARs were calculated from age clusters (note that empty symbols were disregarded for AR calculation), representing short and intense mound development pulses. Age clusters are separated by core intervals that have a very low number of corals ages, indicating a temporary sparse occurrence of CWCs, or by hiatuses (dashed horizontal lines), representing periods of no coral growth (or erosion), leading to a significant slow-down (ARs < 15 cm kyr⁻¹) or stagnation in mound development (indicated by dashed grey bars). (For interpretation of the references to colour in this figure legend, the reader is referred to the Web version of this article.)

ages were obtained and the calculated AR was low with ~6 cm kyr⁻¹. The next two age clusters mainly coincided with the stadial MIS 7d (234−219 ka) and the MIS 7b (209−201 ka), which is a short stadial within the interglacial complex MIS 7a-c (Fig. 3). During MIS 7d the calculated AR was rather low with ~17 cm kyr⁻¹, while during MIS 7b, the AR was high with 120 cm kyr⁻¹. The MIS 7b age cluster was followed by a hiatus temporally spanning over ~90 kyr. The youngest age cluster (upper 10 core metres) coincided with the stadial MIS 5d (115−108 ka) with a corresponding AR of ~145 cm kyr⁻¹ (Fig. 3).

The **gravity core GeoB18105−1** was collected from the central top of the NW-SE elongated **Elf mound**, which is situated just ~7 km to the east of Dragon mound (Fig. 2a). Ten coral ages were obtained, which ranged from 121.7 ± 0.4 to 106.21 ± 0.4 ka (Table S1 of the Supplementary material). As for Dragon mound, also for Elf mound an age cluster is documented that coincided with the stadial MIS 5d (114−110 ka, AR: ~130 cm kyr⁻¹; Fig. 3).

Gravity core GeoB18120−1 was collected from **Mole mound** (central coral belt; Fig. 2a) in a similarly shallow water depth (249 m depth) as the cores from the southern Dragon and Elf mounds (Table 1). Fifteen coral ages, obtained from this core, ranged in total from 78.0 ± 0.3 to 4.8 ± 0.02 ka (Table S1 of the Supplementary material). A first age cluster (78−71 ka) corresponded to the MIS 5a and the calculated mound AR was

60 cm kyr⁻¹ (Fig. 3). Separated by a hiatus covering a time span of ~60 kyr, a second age cluster (13.9−11.7 ka) coincided with the BA to Early Holocene and revealed a high AR of ~220 cm kyr⁻¹ (Fig. 3). This age cluster followed a sudden drop of the AR to <7 cm kyr⁻¹ until an age of 4.8 ka, which marked the core top.

The **MeBo core GeoB18118−2** was collected from the southern top of **BRI** (332 m), from roughly 100 m deeper depths than all other cores (Table 1; Fig. 2a and b). The coral ages (n = 47) obtained from this core ranged from 482.6 ± 14.5 to 8.3 ± 0.1 ka (Table S1 of the Supplementary material). The three oldest coral ages, which were even more the oldest ages obtained for the entire East Melilla CMP, ranged between 483 and 442 ka (Fig. 3). These ages are followed by a hiatus covering a time span of 55 kyr. A first age cluster with ages in chronological order occurred during the end of MIS 11a (387−364 ka) with a corresponding AR of 60 cm kyr⁻¹. The following hiatus covered the interval from the onset of the glacial period of MIS 10 and lasted for ~40 kyr. This is in complete contrast to the Dragon mound record, for which a mound development period during the MIS 10 has been documented (Fig. 3). The ages of the next two age clusters ranged from 327 to 307 ka and corresponded to the full interglacial of MIS 9e (AR: ~50 cm kyr⁻¹) and the interstadial MIS 9c (AR: ~275 cm kyr⁻¹), while no coral ages were obtained for the stadial MIS 9d. The following hiatus covered an interval of ~65 kyr, encompassing the MIS 9a-b, the entire glacial

period of MIS 8, and the full interglacial MIS 7e. The next two age clusters (age range: 242−209 ka) corresponded to the stadial MIS 7d (AR: ~30 cm kyr^{-1}) and the onset of the next full interglacial (MIS 7c; AR: ~125 cm kyr^{-1}) both separated by a short hiatus of ~10 kyr. During the following ~200 kyr (209−15 ka), only four coral ages were obtained, which plot into the MIS 6 (179 ka, 146 ka, 142 ka) and MIS 5a (78 ka), while no coral ages were obtained for the entire last glacial period. Mound ARs during this 200-kyr-time interval were constantly low (1−3 cm kyr^{-1}). The youngest age cluster ranged from 15.4 to 8.3 ka, hence, corresponding to a time interval lasting from the BA until the end of the Early Holocene, as it has already been documented for several other cores retrieved from the BRI (see also Fink et al., 2013; Fentimen et al., 2020). With respect to the entire MeBo record, only this youngest age cluster (upper 10 core metres) displayed an almost strict chronological age order with a high mound AR of ~140 cm kyr^{-1} (Fig. 3).

Gravity core GeoB18118−1 was collected from the **BRI** at the same position as the MeBo core GeoB18118-2 (Fig. 2a) and was used as a supplement for the upper part of this drill core. The 9-m-long core was dated in very high resolution (n = 54; average sampling interval: ~15 cm) and provided ages ranging from 15.1 ± 0.06 to 8.5 ± 0.04 ka (Table S1 of the Supplementary material), corresponding to the BA to Early Holocene (AR: ~130 cm kyr^{-1}). No coral ages being younger than 8.5 ka were obtained, which is in good agreement with the core-top age (8.3 ka) of the MeBo core GeoB18118-2.

5. Discussion

5.1. Non-synchronous mound initiation in the southern Alborán Sea since the Mid-Pleistocene

The Th/U record obtained from Dragon mound in the southern Alborán Sea is unique as for the first time the base of a large Mediterranean coral mound has been penetrated allowing the dating of its initiation to ~390.5 ± 10 ka (Mid-Pleistocene; Fig. 3). While the deglacial to Holocene mound bases of much smaller coral mounds have occasionally been penetrated by conventional gravity coring (Fink et al., 2012; López Correa et al., 2012; Victorero et al., 2016; Tamborrino et al., 2019), only one other long drill record through a complete mound sequence of 150 m length exists for the Porcupine Seabight in the NE Atlantic (IODP expedition 307; Ferdelman et al., 2006). The base of the prominent Challenger mound record revealed a Late Pliocene age (~2.6−2.7 Ma; Kano et al., 2007; Huvenne et al., 2009), which was likely the initiation date for most of the coral mounds in the Porcupine Seabight (Van Rooij et al., 2003). In addition, based on seismic data, it is assumed that coral mounds on the SW Rockall Trough margin (the tallest mounds discovered worldwide with heights of up to 380 m) initiated in two stages during the Mid-Miocene (after ~16 Ma) and during the Early Pliocene (~3.5−4.5 Ma; Mienis et al., 2006). Hence, the ~60-m-high Dragon mound with its Mid-Pleistocene base age revealed a much shorter life span compared to these large NE Atlantic coral mounds.

Initiation in mound formation occurred non-synchronous within the East Melilla CMP as the MeBo core retrieved from the BRI, yielded coral fragments with an age of ~482.6 ± 15 ka (at ~66 m drill depth; Fig. 3), even though possibly less than ~50% of the coral ridge were drilled as it has a total height of ~140 m rising from 470 to 330 m water depth (Fig. 2a and b; Hebbeln et al., 2015). Although there is still no information on the true nature of the basement of the ridge (Hebbeln, 2019), a first preliminary estimation of the initiation time of BRI is provided here: Considering that the upper ~66 m of BRI developed during a time span of ~460−490 kyr with an average AR of ~70 cm kyr^{-1}, and applying this AR to the lower

part of the coral ridge (~74 m; assuming that the mound is entirely formed by CWC and has no substantial extension below the seafloor), a base age of ~980−1040 ka is speculated. Hence, the formation of BRI possibly initiated during the Mid-Pleistocene Transition (MPT, 1250−700 ka; Clark et al., 2006). This finding correlates well with a seismic study from the Moroccan margin on the Atlantic side of the Strait of Gibraltar, where coral mounds initiated on ten different seismic horizons, which were interpreted to be related to glacial periods since the early MPT (Vandorpe et al., 2017). The MPT is marked by an intensification of climate cycles due to a switch from a dominant low-amplitude 41-kyr (obliquity-related) to a high-amplitude 100-kyr (eccentricity-related) orbital periodicity (Clark et al., 2006). As a consequence, ice age cycles became distinctly asymmetrical with strong glacials causing a gradual increase of the global ice volume and decrease of deep-water temperatures, which affected many other components of the climate system (e.g., deep-water formation, ocean circulation, monsoon intensity; Clark et al., 2006; Chalk et al., 2017). Hence, the more extremely variable conditions between interglacial complexes and glacial periods seem to have set the scene for coral mound initiation and subsequent development on both sides of the Strait of Gibraltar since the MPT. Climate-induced environmental changes during the MPT are assumed to have also played an important role in the evolution of the Challenger mound in the NE Atlantic, as a re-initiation in mound development of this coral mound started at ~1000 ka following a major hiatus lasting for ~700 kyr (Kano et al., 2007; Titschack et al., 2009).

5.2. Coral mound development in the Alborán Sea during the last 480 kyr

The MeBo drill records obtained from the Dragon mound and the BRI revealed that CWCs populated the coral mounds in the southern Alborán Sea for ~480 kyr (and presumably even for ~1000 kyr, when considering the extrapolated mound base age of BRI). Both drill cores documented a discontinuous mound formation history with recurring mound development "*pulses*" that lasted for rather short time intervals of 10−30 kyr. The short pulses in mound development were associated with high ARs of >20 cm kyr^{-1} and even up to 275 cm kyr^{-1}. These ARs were much higher as those obtained for the Cabliers mound (20−40 cm kyr^{-1}; Fig. 4), situated 50 km to the north of the East Melilla CMP (Fig. 1b), which vertically grew by only 10 m within ~370 kyr (Corbera et al., 2021). The ARs of the East Melilla mounds were also considerably higher as ARs revealed by the Challenger mound record in the NE Atlantic (1−13 cm kyr^{-1}; Kano et al., 2007). The comparatively high ARs explain why the coral mounds of the East Melilla CMP reached such remarkable dimensions (up to 140 m in height), even though they revealed much shorter life spans (~0.5−1 Ma) compared to their NE Atlantic counterparts (~2.6−4.5 Ma; Mienis et al., 2006; Kano et al., 2007).

Combined with the shorter core records obtained from other mounds in the area (this study; Corbera et al., 2021) some distinct inter-mound variability has been identified. After its initiation at ~390 ka, the shallow Dragon mound experienced a rapid and quasi-continuous aggradation period, which persisted throughout the following 90 kyr with peak ARs during the glacial period of the MIS 10 and during the MIS 9b-d (Fig. 3). Between 390 and 300 ka, the mound reached already a height of >30 m, hence more than 50% of its present-day elevation. The BRI, located ~15 km to the north of Dragon mound at ~100 m deeper waters, was also growing by about ~30 m in height between ~390 and 310 ka. But in contrast to the Dragon mound record, there is an apparent lack of coral deposits corresponding to the glacial period of MIS 10. This lack is probably due to unfavourable environmental conditions hampering coral
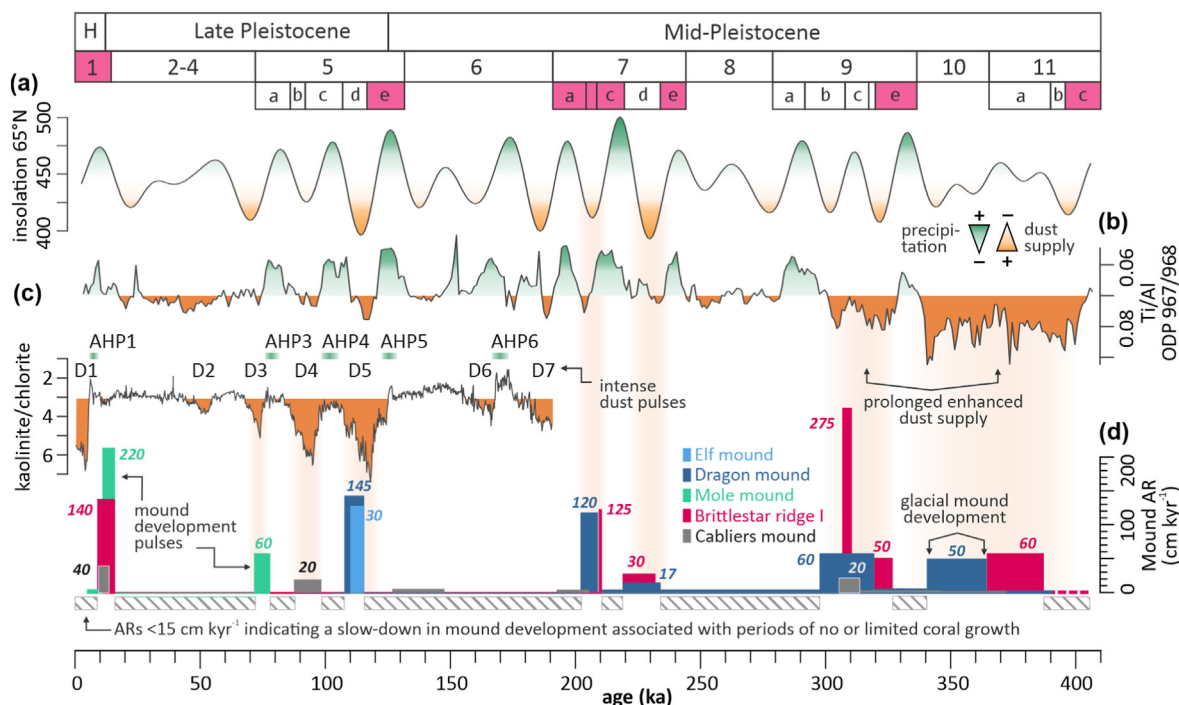
Fig. 4. (**a**) Summer (21 June) insolation curve for 65°N (Laskar et al. 2004). Insolation maxima (green peaks) indicated times of intensified African monsoon precipitation (e.g., Grant et al. 2017), insolation minima (orange peaks) indicate times of enhanced dust supply from the Sahara and northern Africa (e.g., Ehrmann et al. 2017; Sabatier et al. 2020). (**b**) Ti/Al ratio of the composite ODP 967/968 record (Levantine Basin). The Ti/Al in the sediments at these ODP sites is considered to be determined by two major sources, the Nile river suspended matter (depleted in titanium) and windblown dust (enriched in titanium). The Ti/Al changes are therefore linked to monsoonal-induced humidity changes in central to northern Africa (Ziegler et al. 2010; Konijnendijk et al. 2014). (**c**) Influx of clay-sized Saharan dust to the Mediterranean Sea as expressed by the kaolinite/chlorite ratios in a sediment core collected off the Libyan coast. Intense dust pulses (orange peaks) following African Humid Periods (AHP) are labelled D1-D7 (Ehrmann and Schmiedl 2021). Dust pulses D3 − D5 coincided with pronounced mound development pulses during the last interglacial. (**d**) Mound aggradation rates (ARs) calculated for the East Melilla mounds and one Cabliers mound (MD13-3469G, water depth: 417 m; Corbera et al. 2021). ARs of > 15 cm kyr^{-1} (and up to 220 cm kyr^{-1}) are interpreted to represent periods of enhanced mound development, while ARs of < 15 cm kyr^{-1} correspond to times without or limited coral growth that led to a slow-down or stagnation in mound development (AR threshold according to Frank et al. 2009). (For interpretation of the references to colour in this figure legend, the reader is referred to the Web version of this article.)

growth at this deepest site during the MIS 10, although also mass wasting cannot entirely be excluded. Further significant differences in the formation pattern among the mounds in the southern Alborán Sea occurred since the MIS 5. The last mound development pulse documented for the Dragon mound occurred during the stadial MIS 5d, when this mound grew by about 10 m within 7 kyr. Interestingly, this final mound development pulse is also displayed in the record of the neighbouring Elf mound. As this development pulses ended for both mounds at ~108−110 ka, it is rather unlikely that this is a random pattern caused by mass wasting. Instead, we assume a decline in coral growth induced by environmental changes that affected both shallow East Melilla mounds occurring in the same water depth (~230 m) and in close proximity (~7 km). This led to the cessation in mound development, with both mounds remaining in a dormant state until today. The exposed fossil corals lack a cover of hemipelagic sediments, which might be related to accelerated currents that prevented the deposition of fine sediment particles on their summit areas (*sensu* van der Kaaden et al., 2021). Indeed, deep moats and drift sediments surrounding all East Melilla mounds (Figs. 1 and 2) are clear indicators for a highly dynamic environment in which the mounds developed. Overall, the on-mound exposure of fossil corals without a significant cover of hemipelagic sediments seems to be a common phenomenon. It has also been documented for many other dormant mounds in the Atlantic, for which coral ages at the mound top have been reported, ranging from a few kiloyears (off Brazil, Morocco, Namibia; Mangini et al., 2010; Wienberg et al., 2010; Tamborrino et al., 2019) to up to ~108 ka (off Mauritania; Wienberg et al., 2018).

The core retrieved from Mole mound (Fig. 2a) documented a short mound development pulse during the MIS 5a (78−71 ka), and the Cabliers mound in the north of the East Melilla CMP displayed a development pulse coinciding with the MIS 5b-c (99−88 ka; Corbera et al., 2021), which falls temporally between the mound-forming pulses observed for Dragon/Elf and Mole mound (Fig. 4). In contrast, no mound development pulse during the MIS 5 is documented in the MeBo core obtained from the BRI. The ridge also appears to have remained in a "near"-dormant state during the previous MIS 6 and the following glacial period. During this very long time-span of ~200 kyr (210−15 ka), the coral ridge grew only by about 6 m likely related to a sparse occurrence of CWCs (e.g., small, scattered colonies on the mound).

Moreover, it seems likely that during the last glacial period (MIS 2−4), CWCs were (almost completely) absent on the BRI as well as on other coral mounds in the region (Dragon, Elf, Mole, Cabliers) as evidenced by the apparent lack of coral ages for this cold climate period (except of one single age from Mole mound; Fig. 3). Hence, a long-lasting period with limited or without coral growth, which resulted in a marked slow-down and even stagnation in mound development during the last glacial, seems to be a general phenomenon in the southern Alborán Sea that had long remained speculative due to the lack of suitable core material (see Fink et al., 2015).

Following this pronounced glacial interruption in mound development, the BRI had its most recent development pulse during the last deglaciation to Early Holocene (Fig. 3), which is well-documented for all cores obtained from BRI (Fink et al., 2013;

Stalder et al., 2018; Fentimen et al., 2020; this study), and was also found for Mole mound, two further coral mounds of the central mound belt in the East Melilla CMP (Serpent and Horse mounds, Fig. 2a; Stalder et al., 2015; Stalder et al., 2018), and for the Cabliers mound in the north (Corbera et al., 2021).

5.3. Environmental controls on coral mound development in the southern Alborán Sea

The vitality of CWCs directly depends on the local ambient environmental conditions (e.g., water temperature, oxygen concentrations, pH, food controlled by surface productivity and turbulent bottom currents; Davies and Guinotte, 2011). In turn, the development of coral mounds not just requires vivid CWC reefs, but also the concurrent supply of terrigenous sediments, which derive from fluvial or aeolian input but also from iceberg discharge, and are delivered or resuspended by moderate to strong bottom currents (e.g., Pirlet et al., 2011). Since an energetic hydrodynamic regime commonly prevails on top of a coral mound (Dorschel et al., 2007b; Mohn et al., 2014; Cyr et al., 2016; Juva et al., 2020; van der Kaaden et al., 2021), bypassing suspended sediments only become deposited when large and densely distributed coral (reef) frameworks are present, as those have the capability to reduce the velocity of near-bottom currents allowing sediment deposition between their branches (baffling; Huvenne et al., 2009; Titschack et al., 2009; Wang et al., 2021). Moreover, a flourishing reef needs the stabilising effect of a sediment infill for preventing successive fragmentation (by bioerosion, currents, gravity) and for developing into a mound several tens or even hundreds of metres high. Hence, to unravel the environmental controls which fostered mound development in the past, it is not just necessary to decipher environmental conditions promoting coral growth, but also potential sediment sources and periods of enhanced sediment supply need to be identified.

5.3.1. The missing link between climate oscillations and coral mound development in the southern Alborán Sea

The temporal pattern of mound development documented for the East Melilla coral mounds in the southern Alborán Sea during the last ~480 kyr apparently follows no ice age-paced oscillations. Mound development coincided either with full interglacials (MIS 9e, MIS 11a), stadials (e.g. MIS 5d, MIS 7d) or interstadials (e.g. MIS 5a) of interglacial complexes (MIS substages according to Railsback et al., 2015, definition of interglacials according to Past Interglacials Working Group of PAGES, 2016), but also occurred during the glacial period of MIS 10 as documented for the Dragon mound (Fig. 3). In addition, the most recent mound development stage during the BA and Early Holocene, which is documented in all core records obtained from mounds in the southern Alborán Sea (except of Dragon and Elf mound; e.g., Fink et al., 2015; Stalder et al., 2018; Wang et al., 2019; Fentimen et al., 2020; Corbera et al., 2021; our study), is the only one, whose onset coincided with one of the major glacial terminations during the last 480 kyr (Fig. 3).

This is in contrast to what is reported for coral mounds in the NE Atlantic Ocean, where mound development in the northern NE Atlantic (off NW Europe) occurred primarily during warm climate periods (e.g., Dorschel et al., 2007a; Frank et al., 2009; López Correa et al., 2012; van der Land et al., 2014; Wienberg et al., 2020), while mound development was largely restricted to glacial periods in the warm-temperate to sub-tropical NE Atlantic (off NW Africa; Foubert et al., 2008; Wienberg et al., 2010; Eisele et al., 2011; Wienberg et al., 2018). These synchronous north-south oscillations of the biogeographic limits of coral mound development have been related to shifts of the polar front that caused north-south displacements of cold and nutrient-rich intermediate waters (Frank

et al., 2011). However, since such an ice age-paced pattern (matching the 100-kyr cycle in eccentricity) is obviously less clear for the southern Alborán Sea, and also, since mound development only occurred as short pulses with a duration of only ~10−30 kyr (Figs. 3 and 4), environmental processes changing on shorter timescales must have had a more significant influence on the development of the coral mounds in the southern Alborán Sea.

5.3.2. The influence of changes in African continental hydroclimate on coral mound development in the southern Alborán Sea

The Mediterranean Sea is located at the boundary between two climate regimes, and therefore responds very sensitive and quickly to changes in atmospheric forcing and hydroclimate in adjacent continents (Alpert et al., 2006; Lionello et al., 2006). Its northern part represents a maritime coastal climate, dominated by westerlies and influenced by the North Atlantic Oscillation (e.g., Hurrell, 1995; Wassenburg et al., 2016), while its southern part is characterised by a subtropical desert climate, dominated by trade winds and influenced by the descending branch of the Hadley cell (e.g., Chylek et al., 2001; Giraudi, 2005). Moreover, the Mediterranean Sea is influenced by two important monsoon systems, namely the South Asian and the African monsoons, which control precipitation, vegetation cover, dust mobilisation and river discharge in the region (Alpert et al., 2006). All these climate phenomena regulate the climate of the Mediterranean region, and also affect the thermohaline circulation structure, deep-water formation, surface productivity and the heat balance of the Mediterranean Sea, thus significantly impacting marine ecosystems (e.g., Durrieu de Madron et al. 2011; Josey et al., 2011; Kim et al., 2019).

During the Late Quaternary, precessional variations of the Earth's orbit (with a cyclicity of ~23 kyr) exerted regular north-south shifts of the Inter Tropical Convergence Zone (ITCZ) and the African monsoon system (Rossignol-Strick, 1985; Rohling et al., 2002; Larrasoaña et al., 2003; Ziegler et al., 2010), resulting in major hydrological changes in northern Africa (Gasse, 2000; Lézine et al., 2011; McGee et al., 2013; Tierney et al., 2017). During boreal summer insolation maxima of the northern hemisphere, the ITCZ and the tropical rainbelt moved northward over the continent. The enhanced precipitation over northern Africa turned regions, which were formerly characterised by deserts, into areas covered by river systems (Fig. 1a), lakes and dense vegetation (African Humid Periods, AHPs) (e.g., deMenocal et al., 2000; Gasse, 2000; Tjallingii et al., 2008; Lézine et al., 2011; Grant et al., 2017; Blanchet et al., 2021). Conversely, during boreal summer insolation minima, the ITCZ and the monsoon rain belt moved southward (e.g., Tjallingii et al., 2008; Lézine et al., 2011). This caused a desertification of the Sahara and northern Africa, resulting in increased aeolian dust transport as commonly documented in marine and lacustrine sediments of the Mediterranean region (e.g., Larrasoaña et al., 2003; Bout-Roumazeilles et al., 2007; Revel et al., 2010; Rodrigo-Gámiz et al., 2011; Ehrmann et al., 2017; Sabatier et al., 2020; Blanchet et al., 2021). We propose that this had two potentially positive effects on coral mound development: (i) enhanced productivity triggered by dust fertilisation supported CWC growth (see also Wienberg et al., 2010), and (ii) high dust fluxes delivered sufficient sediments to stabilize the reef structure and to significantly contribute to the mound volume, thereby promoting enhanced mound aggradation (e.g., Roberts et al., 2006; Huvenne et al., 2009; Wienberg and Titschack, 2017). Indeed, we found an intriguing temporal correlation of the mound development pulses documented for the southern Alborán Sea with enhanced fluxes of aeolian dust towards the Mediterranean (Fig. 4). Most convincing is the correlation with intense dust pulses recently documented for the MIS 5 (starting after the termination of the strong Eemian AHP5) with each lasting for only 10−14 kyr (D5 - D3; Ehrmann and

Schmiedl, 2021), which temporally coincided almost perfectly with the mound development pulses documented for the Dragon/Elf, Mole, and Cabliers mounds lasting for similarly short time intervals (~7−15 kyr; Fig. 4). Immediately after the abrupt termination of AHPs, these dust pulses delivered high loads of sediments from desiccated soils, lake and river beds towards the Mediterranean Sea. Their intensity was directly proportional to the monsoon intensity steering the preceding AHP as more weathering products were formed and mobilised by wind erosion after desiccation, while the dust transport decreased successively to a stable background level when the main dust sources became exhausted (Ehrmann et al., 2017; Ehrmann and Schmiedl, 2021). The fact that the dust pulses during the MIS 5 triggered mound formation only at one specific site might be related to the depth of the mounds, their distance to the continent, or yet unidentified (local) oceanographic processes.

Moreover, a prolonged period of increased dust flux was documented in sediments of the Mediterranean Sea, lasting from ~400 to 300 ka (MIS 11c to MIS 9b) and interrupted only by a brief period of more humid conditions between ~338 and 330 ka (related to an insolation maximum during the first part of the interglacial MIS 9a; Fig. 4; Konijnendijk et al., 2014). This correlates perfectly with the mound development pattern documented for the East Melilla CMP and likely explains the rapid vertical aggradation of the Dragon mound and the BRI of about 30 m within this 100-kyr-time interval during the Mid-Pleistocene (Figs. 3 and 4). However, while Dragon mound continued to grow during the glacial period of the MIS 10, the record of the deeper BRI shows a distinct hiatus at the same time (Fig. 4). Considering this hiatus was related to an interruption in coral growth on BRI 10 during the MIS10, this contrasting pattern might be related to the depth of the mounds and/or their distance from the African continent. Dragon mound, located at ~230 m depth just ~15 km north of the Moroccan shelf edge, might have profited from specific glacial conditions prevailing close to the shelf. For example, enhanced offshore winds may have intensified cyclonic circulation and Ekman pumping, resulting in locally enhanced productivity and/or a shoaling of the pycnocline between the LIW and Atlantic water (Myers et al., 1998; Jouet et al., 2006; Rohling et al., 2015). However, further research is needed to substantiate such speculations.

Our data revealed a strong correlation between increased dust supply and mound development in the southern Alborán Sea, although it was apparently not the only trigger since there are few deviations from the proposed pattern. Times of high dust supply that are documented for the last three glacial periods (e.g., dust pulses D2 during MIS2-4 and D6/7 during MIS 6; Ehrmann and Schmiedl, 2021) did not result in enhanced mound development, probably related to a low abundance of CWCs (Figs. 3 and 4). And even more astonishing, a very intense dust pulse (D1 in Fig. 4; Ehrmann and Schmiedl, 2021) following the termination of the last AHP was also not accompanied by mound development. Thus, although high productivity conditions induced by the fertilisation effect of the supplied dust should have favoured the growth of CWC, other environmental factors (e.g., temperature, oxygen) and oceanographic processes (e.g., ocean circulation, bottom currents, turbulence) hampered their proliferation preventing them from forming large reefs on the coral mounds in the southern Alborán Sea. Further, we should also consider species-specific effects. The strong reduction in mound ARs since the Early Holocene coincided with an apparent change from *D. pertusum*-to *M. oculata*-dominated coral (mound) communities (Stalder et al. 2015, 2018; Fentimen et al., 2020; Corbera et al., 2021). This was previously linked to the sudden and strong increase in water temperatures since the BA interstadial (Wienberg, 2019), to which *M. oculata* appears to be more resilient (Wienberg and Titschack, 2017).

However, due to its limited ability to form large frameworks (Roberts et al., 2009; Orejas et al., 2021), this species may be less successful at maintaining mound development (Wienberg, 2019).

5.3.3. The importance of hydrodynamic processes on Mediterranean coral mound development

Today, the well-ventilated and nutrient-rich LIW appears to be an important oceanographic component conditioning a suitable environment for CWCs, as evidenced by the present-day link between its flow path and the occurrence of living CWCs (e.g., Taviani et al., 2017). Moreover, it has been suggested that internal wave activity at the interface between the LIW and overlying Atlantic waters, and its positive effect of increasing turbulence and food/sediment supply, supported the latest CWC bloom and associated mound development pulse during the last deglaciation (Wang et al., 2019; Corbera et al., 2021). The flow depth of the LIW in the western Mediterranean has fluctuated repeatedly, e.g. induced by sea-level changes during the last 130 kyr (Toucanne et al., 2012), and it is likely that the deepening/shoaling of the LIW has also caused a vertical shift of associated internal waves (Rodrigo-Gámiz et al., 2011; Ercilla et al., 2016). Such vertical shifts would have resulted in CWC reefs thriving on the coral mounds of the Alborán Sea being in and out of optimal (hydrodynamic) environmental conditions, a scenario which has previously been described for coral mounds on the Irish margin (Wienberg et al., 2020). Moreover, also the amplitude of internal waves could have varied over time, due to variations in the LIW flow.

This brings us back to the African hydrology as changes in continental hydroclimate can affect the flow depth and intensity of the LIW. A dry and warm climate in combination with a reduced freshwater input from rivers favours the formation of dense LIW (Lascaratos et al., 1999; Schroeder et al., 2017). In contrast, increased precipitation over northern Africa during AHPs is commonly accompanied by intensified fluvial freshwater discharge via the Nile river, via palaeo-river systems flowing northward from the central Saharan watershed into the Ionian Sea (Gulf of Sirte; e.g., Blanchet et al., 2021), and probably also via numerous smaller rivers along the Moroccan, Algerian and Tunisian coasts draining from the Atlas Mountains into the western Mediterranean basin (Fig. 1a). An increased freshwater input would led to decreased surface water salinity and enhanced water-mass stratification, which impairs LIW and deep-water formation in the eastern Mediterranean basin (e.g., Bethoux and Gentili, 1999; Revel et al., 2010; Toucanne et al., 2012; Bahr et al., 2015; Rohling et al., 2015; Tesi et al., 2017; Kaboth-Bahr et al., 2018). Indeed, strong decreases in mound ARs regularly coincided with the onset of AHPs marked by increased precipitation (during insolation maxima in Fig. 4). Hence, increased freshwater input during AHPs and its implications on the ventilation and thermohaline circulation patterns in the Mediterranean Sea as well as on the formation and vertical range of internal waves may therefore have adversely affected the Mediterranean CWC communities by providing low-energetic and oxygen-depleted conditions at intermediate to deep depths (see also Fink et al., 2012). Such a scenario could also explain the temporal differences in mound development between individual mounds observed during the MIS 5 (see above; Fig. 4). Variations in the freshwater input, even during relatively dry periods, might have caused vertical shifts of the LIW-Atlantic Water interface and associated internal waves; thus, optimal conditions for mound development may have prevailed only in limited water depth windows. So far, however, suitable paleoceanographic records for the southern Alborán Sea are still lacking that provide information on hydrodynamic changes at intermediate depths during the last ~480 kyr, and could confirm the positive link between past LIW flow and mound development.

6. Conclusions

The here presented MeBo drill core records obtained from the East Melilla CMP significantly expand our knowledge of coral mound initiation and mound development in the western Mediterranean Sea during the last ~480 kyr. The base of a 60-m-high mound has been dated to the Mid-Pleistocene (~390 ka), and it has been shown that mound initiation was non-synchronous, as larger mounds may have initiated already since the MPT (at ~1000 ka). Mound development in the southern Alborán Sea, associated with high ARs of up to 275 cm kyr^{-1}, was restricted to relatively short time intervals (10−30 kyr) that could not be assigned to any ice age-paced climatic oscillation. Instead, our data demonstrate that hydrological changes of the northern African continental climate had an evident remote control on coral mound development in the western Mediterranean Sea. Increased dust supply during dry periods on the northern African continent affected surface productivity and sediment supply, while increased freshwater input during humid periods, altered the intensity and depth of the LIW flow and associated turbulent internal wave activity. The combined influence of changes in productivity, sediment supply and hydrodynamic processes had likely a strong impact on CWC proliferation and on mound development. Land-atmosphere-ocean feedback processes imposed by hydroclimate changes (e.g., Pausata et al., 2020) are especially amplified in the small and semi-enclosed Mediterranean Sea placed between two climate regimes. As a result, its deep-sea ecosystems are likely to be very sensitive to past and future climate change, pointing to a greater vulnerability compared to their Atlantic counterparts.

Author statement

CW led the writing of the manuscript and conceived the study together with DH and NF. DH developed together with DVR and CW the idea and proposal for the MeBo drilling campaign. DH and CW coordinated the scientific cruise and planned the MeBo drilling and gravity coring, and CW coordinated the on-board core processing. TK and HW organised the coral sample collection and the preparation of the sampling material. TK performed together with NF the technical data analyses and quality check (U/Th dating). CW wrote the first draft and prepared all of the figures and tables. All authors provided support to interpret the results and contributed to the final version of the manuscript.

Declaration of competing interest

The authors declare that they have no known competing financial interests or personal relationships that could have appeared to influence the work reported in this paper.

Data availability

Data are archived at the World Data Center PANGAEA. DOI's are mentioned in the suppl. Material

Acknowledgements

Appendix A. Supplementary data

Supplementary data to this article can be found online at https://doi.org/10.1016/j.quascirev.2022.107723.

References

Addamo, A.M., Vertino, A., Stolarski, J., García-Jiménez, R., Taviani, M., Machordom, A., 2016. Merging scleractinian genera: the overwhelming genetic similarity between solitary *Desmophyllum* and colonial *Lophelia*. BMC Evol. Biol. 16, 108.

Alpert, P., Baldi, M., Ilani, R., Krichak, S., Price, C., Rodó, X., Saaroni, H., Ziv, B., Kishcha, P., Barkan, J., Mariotti, A., Xoplaki, E., 2006. Chapter 2 Relations between climate variability in the Mediterranean region and the tropics: ENSO, South Asian and African monsoons, hurricanes and Saharan dust. In: Lionello, P., Malanotte-Rizzoli, P., Boscolo, R. (Eds.), Developments in Earth and Environmental Sciences. Elsevier, pp. 149−177.

Amitai, Y., Ashkenazy, Y., Gildor, H., 2021. The effect of the source of deep water in the eastern Mediterranean on western Mediterranean intermediate and deep water. Front. Mar. Sci. 7, 615975.

Ammar, A., Mauffret, A., Gorini, C., Jabour, H., 2007. The tectonic structure of the Alboran Margin of Morocco. Rev. Soc. Geol. Espana 20, 247−271.

Angeletti, L., Castellan, G., Montagna, P., Remia, A., Taviani, M., 2020. The "Corsica Channel cold-water coral province" (Mediterranean sea). Front. Mar. Sci. 7.

Bahr, A., Kaboth, S., Jiménez-Espejo, F.J., Sierro, F.J., Voelker, A.H.L., Lourens, L., Röhl, U., Reichart, G.J., Escutia, C., Hernández-Molina, F.J., Pross, J., Friedrich, O., 2015. Persistent monsoonal forcing of mediterranean Outflow water dynamics during the late Pleistocene. Geology 43, 951−954.

Bethoux, J.P., Gentili, B., 1999. Functioning of the Mediterranean Sea: past and present changes related to freshwater input and climate changes. J. Mar. Syst. 20, 33−47.

Bethoux, J.P., Gentili, B., Morin, P., Nicolas, E., Pierre, C., Ruiz-Pino, D., 1999. The Mediterranean Sea: a miniature ocean for climatic and environmental studies and a key for the climatic functioning of the North Atlantic. Prog. Oceanogr. 44, 131−146.

Blanchet, C.L., Osborne, A.H., Tjallingii, R., Ehrmann, W., Friedrich, T., Timmermann, A., Brückmann, W., Frank, M., 2021. Drivers of river reactivation in North Africa during the last glacial cycle. Nat. Geosci. 14, 97−103.

Bonneau, L., Colin, C., Pons-Branchu, E., Mienis, F., Tisnérat-Laborde, N., Blamart, D., Elliot, M., Collart, T., Frank, N., Foliot, L., Douville, E., 2018. Imprint of Holocene climate variability on cold-water coral reef growth at the SW Rockall Trough Margin, NE Atlantic. G-cubed 19, 2437−2452.

Border, E.C., 2020. Variability of $\delta^{234}U$ in the Mediterranean Sea, Amazon Estuary, and Atlantic Ocean. PhD Ph.D. thesis. Heidelberg University, p. 124. doi: 110.11588/heidok.00028744.

Bout-Roumazeilles, V., Combourieu Nebout, N., Peyron, O., Cortijo, E., Landais, A., Masson-Delmotte, V., 2007. Connection between south mediterranean climate and north African atmospheric circulation during the last 50,000yrBP North Atlantic cold events. Quat. Sci. Rev. 26, 3197−3215.

Chalk, T.B., Hain, M.P., Foster, G.L., Rohling, E.J., Sexton, P.F., Badger, M.P.S., Cherry, S.G., Hasenfratz, A.P., Haug, G.H., Jaccard, S.L., Martínez-García, A., Pälike, H., Pancost, R.D., Wilson, P.A., 2017. Causes of ice age intensification across the Mid-Pleistocene Transition. Proc. Natl. Acad. Sci. USA 114, 13114−13119.

Cheng, H., Lawrence Edwards, R., Shen, C.-C., Polyak, V.J., Asmerom, Y., Woodhead, J., Hellstrom, J., Wang, Y., Kong, X., Spötl, C., Wang, X., Calvin Alexander, E., 2013. Improvements in 230Th dating, 230Th and 234U half-life values, and U−Th isotopic measurements by multi-collector inductively coupled plasma mass

spectrometry. Earth Planet Sci. Lett. 371—372, 82—91.

Chimienti, G., Bo, M., Taviani, M., Mastrototaro, F., 2019. Occurrence and biogeography of Mediterranean cold-water corals. In: Orejas, C., Jiménez, C. (Eds.), Mediterranean Cold-Water Corals: Past, Present and Future, Springer Series: Coral Reefs of the World Vol 9. Springer, pp. 213—243.

Chylek, P., Lesins, G., Lohmann, U., 2001. Enhancement of dust source area during past glacial periods due to changes of the Hadley circulation. J. Geophys. Res. Atmos. 106, 18477—18485.

Clark, P.U., Archer, D., Pollard, D., Blum, J.D., Rial, J.A., Brovkin, V., Mix, A.C., Pisias, N.G., Roy, M., 2006. The middle Pleistocene transition: characteristics, mechanisms, and implications for long-term changes in atmospheric pCO2. Quat. Sci. Rev. 25, 3150—3184.

Comas, M., Pinheiro, L.M., 2007. Discovery of Carbonate Mounds in the Alboran Sea: the Melilla Mound Field. Abstract for the First MAPG International Convention, Conference & Exhibition Marrakech Convention. Center October 28 - 31 2007.

Comas, M., Pinheiro, L.M., Ivanov, M., TTR-17 Scientific Parety, 2009. Deep-water Coral Mounds in the Alboran Sea: the Melilla Mound Field Revisited. In: Comas, M, Suzyumov, A. (Eds.), Geo-Marine Research on the Mediterranean and European-Atlantic Margins International Conference and TTR-17 Post-Cruise Meeting of the Training-through-Research Programme. IOC Workshop Report No. 220, UNESCO, pp. 8—9.

Corbera, G., Lo Iacono, C., Gràcia, E., Grinyó, J., Pierdomenico, M., Huvenne, V.A.I., Aguilar, R., Gili, J.M., 2019. Ecological characterisation of a mediterranean cold-water coral reef: Cabliers coral mound province (Alboran sea, western mediterranean). Prog. Oceanogr. 175, 245—262.

Corbera, G., Lo Iacono, C., Standish, C.D., Gràcia, E., Ranero, C., Anagnostou, E., Huvenne Vait, J., Foster, G.L., 2022. Glacial-aged development of the Tunisian Coral Mound Province controlled by glacio-eustatic oscillations and changes in surface productivity. Mar. Geol. 446, 106772.

Corbera, G., Lo Iacono, C., Standish, C.D., Anagnostou, E., Titschack, J., Katsamenis, O., Cacho, I., Van Rooij, D., Huvenne, V.A.I., Foster, G.L., 2021. Glacio-eustatic variations and sapropel events as main controls on the middle Pleistocene-holocene evolution of the Cabliers coral mound province (W mediterranean). Quat. Sci. Rev. 253, 106783.

Cyr, F., van Haren, H., Mienis, F., Duineveld, G., Bourgault, D., 2016. On the influence of cold-water coral mound size on flow hydrodynamics, and vice versa. Geophys. Res. Lett. 43, 775—783.

Davies, A.J., Guinotte, J.M., 2011. Global habitat suitability for framework-forming cold-water corals. PLoS One 6, e18483.

Davies, A.J., Duineveld, Gerard C.A., Lavaleye, Marc S.S., Bergman, Magda J.N., van Haren, H., Roberts, J.M., 2009. Downwelling and deep-water bottom currents as food supply mechanisms to the cold-water coral *Lophelia pertusa* (Scleractinia) at the Mingulay Reef Complex. Limnol. Oceanogr. 54, 620—629.

deMenocal, P., Ortiz, J., Guilderson, T., Adkins, J., Sarnthein, M., Baker, L., Yarusinsky, M., 2000. Abrupt onset and termination of the African Humid Period: rapid climate responses to gradual insolation forcing. Quat. Sci. Rev. 19, 347—361.

Dorschel, B., Hebbeln, D., Rüggeberg, A., Dullo, W.-C., 2005. Growth and erosion of a cold-water coral covered carbonate mound in the Northeast Atlantic during the Late Pleistocene and Holocene. Earth Planet Sci. Lett. 233, 33—44.

Dorschel, B., Hebbeln, D., Rüggeberg, A., Dullo, W.-C., 2007a. Carbonate budget of a cold-water coral carbonate mound: Propeller Mound, Porcupine Seabight. Int. J. Earth Sci. 96, 73—83.

Dorschel, B., Hebbeln, D., Foubert, A., White, M., Wheeler, A.J., 2007b. Hydrodynamics and cold-water coral facies distribution related to recent sedimentary processes at Galway Mound west of Ireland. Mar. Geol. 244, 184—195.

Douarin, M., Elliot, M., Noble, S.R., Sinclair, D., Henry, L.-A., Long, D., Moreton, S.G., Murray Roberts, J., 2013. Growth of north-east Atlantic cold-water coral reefs and mounds during the Holocene: a high resolution U-series and 14C chronology. Earth Planet Sci. Lett. 375, 176—187.

Durrieu de Madron, X., Guieu, C., Sempéré, R., Conan, P., Cossa, D., D'Ortenzio, F., Estournel, C., Gazeau, F., Rabouille, C., Stemmann, L., Bonnet, S., Diaz, F., Koubbi, P., Radakovitch, O., Babin, M., Baklouti, M., Bancon-Montigny, C., Belviso, S., Bensoussan, N., Bonsang, B., Bouloubassi, I., Brunet, C., Cadiou, J.F., Carlotti, F., Chami, M., Charmasson, S., Charrière, B., Dachs, J., Doxaran, D., Dutay, J.C., Elbaz-Poulichet, F., Eléaume, M., Eyrolles, F., Fernandez, C., Fowler, S., Francour, P., Gaertner, J.C., Galzin, R., Gasparini, S., Ghiglione, J.F., Gonzalez, J.L., Goyet, C., Guidi, L., Guizien, K., Heimbürger, L.E., Jacquet, S.H.M., Jeffrey, W.H., Joux, F., Le Hir, P., Leblanc, K., Lefèvre, D., Lejeusne, C., Lemé, R., Loÿe-Pilot, M.D., Mallet, M., Méjanelle, L., Mélin, F., Mellon, C., Mérigot, B., Merle, P.L., Migon, C., Miller, W.L., Mortier, L., Mostajir, B., Mousseau, L., Moutin, T., Para, J., Pérez, T., Petrenko, A., Poggiale, J.C., Prieur, L., Pujo-Pay, M., Pulido, V., Raimbault, P., Rees, A.P., Ridame, C., Rontani, J.F., Ruiz Pino, D., Sicre, M.A., Taillandier, V., Tamburini, C., Tanaka, T., Taupier-Letage, I., Tedetti, M., Testor, P., Thébault, H., Thouvenin, B., Touratier, F., Tronczynski, J., Ulses, C., Van Wambeke, F., Vantrepotte, V., Vaz, S., Verney, R., 2011. Marine ecosystems' responses to climatic and anthropogenic forcings in the Mediterranean. Prog. Oceanogr. 91, 97—166.

Ehrmann, W., Schmiedl, G., 2021. Nature and dynamics of North African humid and dry periods during the last 200,000 years documented in the clay fraction of Eastern Mediterranean deep-sea sediments. Quat. Sci. Rev. 260, 106925.

Ehrmann, W., Schmiedl, G., Beuscher, S., Krüger, S., 2017. Intensity of African humid periods estimated from Saharan dust fluxes. PLoS One 12, e0170989.

Eisele, M., Frank, N., Wienberg, C., Hebbeln, D., Lopez Correa, M., Douville, E., Freiwald, A., 2011. Productivity controlled cold-water coral growth periods

during the last glacial off Mauritania. Mar. Geol. 280, 143—149.

Eisele, M., Frank, N., Wienberg, C., Titschack, J., Mienis, F., Beuck, L., Tisnerat-Laborde, N., Hebbeln, D., 2014. Sedimentation patterns on a cold-water coral mound off Mauritania. Deep-Sea Res. Part II 99, 307—315.

Eisele, M., Hebbeln, D., Wienberg, C., 2008. Growth history of a cold-water coral covered carbonate mound - Galway Mound, Porcupine Seabight, NE-Atlantic. Mar. Geol. 253, 160—169.

Ercilla, G., Juan, C., Hernández-Molina, F.J., Bruno, M., Estrada, F., Alonso, B., Casas, D., Farran, Ml, Llave, E., García, M., Vázquez, J.T., D'Acremont, E., Gorini, C., Palomino, D., Valencia, J., El Moumni, B., Ammar, A., 2016. Significance of bottom currents in deep-sea morphodynamics: an example from the Alboran Sea. Mar. Geol. 378, 157—170.

Fentimen, R., Feenstra, E., Rüggeberg, A., Vennemann, T., Hajdas, I., Adatte, T., Van Rooij, D., Foubert, A., 2020. Cold-water coral mound archive provides unique insights into intermediate water mass dynamics in the Alboran Sea during the last deglaciation. Front. Mar. Sci. 7. https://doi.org/10.3389/fmars.2020.00354.

Ferdelman, T.G., Kano, A., Williams, T., Henriet, J.P., Scientists, I.E., 2006. Proceedings of the IODP Expedition 307. Modern Carbonate Mounds: Porcupine Drilling. IODP Management International, Washington DC doi:102204/iodpproc3072006.

Fink, H.G., Wienberg, C., De Pol-Holz, R., Hebbeln, D., 2015. Spatio-temporal distribution patterns of Mediterranean cold-water corals (*Lophelia pertusa* and *Madrepora oculata*) during the past 14,000 years. Deep Sea Res. Part I 103, 37—48.

Fink, H.G., Wienberg, C., De Pol-Holz, R., Wintersteller, P., Hebbeln, D., 2013. Cold-water coral growth in the Alboran sea related to high productivity during the late Pleistocene and Holocene. Mar. Geol. 339, 71—82.

Fink, H.G., Wienberg, C., Hebbeln, D., McGregor, H.V., Schmiedl, G., Taviani, M., Freiwald, A., 2012. Oxygen control on Holocene cold-water coral development in the eastern Mediterranean Sea. Deep Sea Res. Part I 62, 89—96.

Foubert, A., Depreiter, D., Beck, T., Maignien, L., Pannemans, B., Frank, N., Blamart, D., Henriet, J.-P., 2008. Carbonate mounds in a mud volcano province of northwest Morocco: key to processes and controls. Mar. Geol. 248, 74—96.

Frank, N., Paterne, M., Ayliffe, L., van Weering, T.C.E., Henriet, J.-P., Blamart, D., 2004. Eastern North Atlantic deep-sea corals: tracing upper intermediate water $\Delta^{14}C$ during the Holocene. Earth Planet Sci. Lett. 219, 297—309.

Frank, N., Ricard, E., Lutringer-Paquet, A., van der Land, C., Colin, C., Blamart, D., Foubert, A., Van Rooij, D., Henriet, J.-P., de Haas, H., van Weering, T., 2009. The Holocene occurrence of cold water corals in the NE Atlantic: implications for coral carbonate mound evolution. Mar. Geol. 266, 129—142.

Frank, N., Freiwald, A., López Correa, M., Wienberg, C., Eisele, M., Hebbeln, D., Van Rooij, D., Henriet, J.P., Colin, C., van Weering, T., de Haas, H., Buhl-Mortensen, P., Roberts, J.M., De Mol, B., Douville, E., Blamart, D., Hatte, C., 2011. Northeastern Atlantic cold-water coral reefs and climate. Geology 39, 743—746.

Frederiksen, R., Jensen, A., Westerberg, H., 1992. The distribution of scleratinian coral *Lophelia pertusa* around the Faroe Islands and the relation to intertidal mixing. Sarsia 77, 157—171.

Freiwald L, Beuck L, Rüggeberg A Taviani M, Hebbeln D, R/V Meteor Cruise M70-1 participants (2009) the white coral community in the central Mediterranean Sea revealed by ROV surveys. Oceanography 22:58-74.

Freudenthal, T., Wefer, G., 2013. Drilling cores on the sea floor with the remote-controlled sea floor drilling rig MeBo. Geosci. Instrum. Methods Data Syst. 2, 329—337.

Gasse, F., 2000. Hydrological changes in the African tropics since the last glacial maximum. Quat. Sci. Rev. 19, 189—211.

Giraudi, C., 2005. Eolian sand in peridesert northwestern Libya and implications for Late Pleistocene and Holocene Sahara expansions. Palaeogeogr. Palaeoclimatol. Palaeoecol. 218, 161—173.

Gori A, Wienberg C, Grinyo J, Taviani M, Hebbeln D, Lo Iacono C, Freiwald A, C. O (accepted) Life and death of cold-water corals across the Mediterranean Sea. In: Cordes E, Mienis F (eds) Cold-Water Coral Reefs of the World. Springer series: Coral Reefs of the World, pp.

Grant, K.M., Rohling, E.J., Westerhold, T., Zabel, M., Heslop, D., Konijnendijk, T., Lourens, L., 2017. A 3 million year index for North African humidity/aridity and the implication of potential pan-African Humid periods. Quat. Sci. Rev. 171, 100—118.

Grant, K.M., Rohling, E.J., Ramsey, C.B., Cheng, H., Edwards, R.L., Florindo, F., Heslop, D., Marra, F., Roberts, A.P., Tamisiea, M.E., Williams, F., 2014. Sea-level variability over five glacial cycles. Nat. Commun. 5, 5076.

Hanz, U., Wienberg, C., Hebbeln, D., Duineveld, G., Lavaleye, M., Juva, K., Dullo, W.-C., Freiwald, A., Tamborrino, L., Reichart, G.-J., Flögel, S., Mienis, F., 2019. Environmental factors influencing cold-water coral ecosystems in the oxygen minimum zones on the Angolan and Namibian margins. Biogeosciences 16, 4337—4356.

Hayes, D.R., Schroeder, K., Poulain, P.-M., Testor, P., Mortier, L., Bosse, A., du Madron, X., 2019. Review of the circulation and characteristics of intermediate water masses of the Mediterranean: implications for cold-water coral habitats. In: Orejas Saco del Valle, C., Jiménez, C. (Eds.), Mediterranean Cold-Water Corals: Past, Present and Future, Springer Series: Coral Reefs of the World. Springer, pp. 195—211.

Hebbeln, D., 2019. Highly variable submarine landscapes in the Alborán Sea created by cold-water corals. In: Orejas Saco del Valle, C., Jiménez, C. (Eds.), Mediterranean Cold-Water Corals: Past, Present and Future, Springer Series: Coral Reefs of the World. Springer, pp. 61—65.

Hebbeln, D., Van Rooij, D., Wienberg, C., 2016. Good neighbours shaped by vigorous currents: cold-water coral mounds and contourites in the North Atlantic. Mar.

Geol. 378, 171—185.

Hebbeln, D., Wienberg, C., Beuck, L., Freiwald, A., Wintersteller, P., cruise partici-pants, 2009. Report and Preliminary Results of RV POSEIDON Cruise POS 385 "Cold-Water Corals of the Alboran Sea (Western Mediterranean Sea)", Faro - Toulon. May 29 - June 16 2009 Reports of the Department of Geosciences (GeoB), University of Bremen. No 273 79.

Hebbeln, D., Wienberg, C., Bartels, M., Bergenthal, M., Frank, N., Gaide, S., Henriet, J.P., Kaszemeik, K., Klar, S., Klein, T., Krengel, T., Kuhnert, M., Meyer-Schack, B., Noorlander, C., Reuter, M., Rosiak, U., Schmidt, W., Seeba, H., Seiter, C., Strange, N., Terhzaz, L., Van Rooij, D., 2015. MoccoMeBo: climate-driven development of Moroccan cold-water coral mounds revealed by MeBo-drilling: Atlantic vs. Mediterranean settings - cruise MSM36 - february 18-March 14, 2014 - Malaga (Spain) - Las Palmas (Spain) MARIA S MERIAN-reports, MSM36. DFG-Senatskomm. Ozeanogr. 47. https://doi.org/10.2312/cr_msm2336.

Heburn, G.W., La Violette, P.E., 1990. Variations in the structure of the anticyclonic gyres found in the Alboran Sea. J. Geophys. Res.: Oceans 95, 1599—1613.

Hennige, S.J., Larsson, A.I., Orejas, C., Gori, A., De Clippele, L.H., Lee, Y.C., Jimeno, G., Georgoulas, K., Kamenos, N.A., Roberts, J.M., 2021. Using the Goldilocks Prin-ciple to model coral ecosystem engineering. Proc. Biol. Sci. 288, 20211260.

Hurrell, J.W., 1995. Decadal trends in the north Atlantic oscillation: regional tem-peratures and precipitation. Science 7, 676—679.

Huvenne, V.A.I., Van Rooij, D., De Mol, B., Thierens, M., O'Donnell, R., Foubert, A., 2009. Sediment dynamics and palaeo-environmental context at key stages in the Challenger cold-water coral mound formation: clues from sediment de-posits at the mound base. Deep Sea Res. Part I 56, 2263—2280.

Josey, S.A., Somot, S., Tsimplis, M., 2011. Impacts of atmospheric modes of variability on Mediterranean Sea surface heat exchange. J. Geophys. Res.: Oceans 116.

Jouet, G., Berné, S., Rabineau, M., Bassetti, M.A., Bernier, P., Dennielou, B., Sierro, F.J., Flores, J.A., Taviani, M., 2006. Shoreface migrations at the shelf edge and Sea-level changes around the last glacial maximum (Gulf of Lions, NW mediterra-nean). Mar. Geol. 234, 21—42.

Juan, C., Ercilla, G., Javier Hernández-Molina, F., Estrada, F., Alonso, B., Casas, D., García, M., Farran, Ml, Llave, E., Palomino, D., Vázquez, J.-T., Medialdea, T., Gorini, C., D'Acremont, E., El Moumni, B., Ammar, A., 2016. Seismic evidence of current-controlled sedimentation in the Alboran Sea during the Pliocene and quaternary: palaeoceanographic implications. Mar. Geol. 378, 292—311.

Juva, K., Flögel, S., Karstensen, J., Linke, P., Dullo, W.-C., 2020. Tidal dynamics control on cold-water coral growth: a high-resolution multivariable study on eastern Atlantic cold-water coral sites. Front. Mar. Sci. 7, 132 doi:110.3389/fmars.2020.00132.

Kaboth-Bahr, S., Bahr, A., Zeeden, C., Toucanne, S., Eynaud, F., Jiménez-Espejo, F., Röhl, U., Friedrich, O., Pross, J., Löwemark, L., Lourens, L.J., 2018. Monsoonal forcing of European ice-sheet dynamics during the late quaternary. Geophys. Res. Lett. 45, 7066—7074.

Kano, A., Ferdelman, T.G., Williams, T., Henriet, J.-P., Ishikawa, T., Kawagoe, N., Takashima, C., Kakizaki, Y., Abe, K., Sakai, S., Browning, E.L., Li, X., 2007. Inte-grated Ocean Drilling Program Expedition 307 Scientists. In: Age Constraints on the Origin and Growth History of a Deep-Water Coral Mound in the Northeast Atlantic Drilled during Integrated Ocean Drilling Program Expedition 307, vol. 35. Geology, pp. 1051—1054.

Kim, G.-U., Seo, K.-H., Chen, D., 2019. Climate change over the Mediterranean and current destruction of marine ecosystem. Sci. Rep. 9, 18813.

Konijnendijk, T.Y.M., Ziegler, M., Lourens, L., 2014. Chronological constraints on Pleistocene sapropel depositions from high-resolution geochemical records of ODP Sites 967 and 968. Newsl. Stratigr. 47.

Korpanty C, Hoffman L, Portilho-Ramos R, Titschack J, Wienberg C, Hebbeln D (submitted) Decline in cold-water coral growth promotes molluscan diversity: a paleontological perspective from a cold-water coral mound in the western Mediterranean Sea. Front. Mar. Sci.

Larrasoaña, J.C., Roberts, A.P., Rohling, E.J., Winklhofer, M., Wehausen, R., 2003. Three million years of monsoon variability over the northern Sahara. Clim. Dynam. 21, 689—698.

Lascaratos, A., Roether, W., Nittis, K., Klein, B., 1999. Recent changes in deep water formation and spreading in the eastern Mediterranean sea: a review. Prog. Oceanogr. 44, 5—36.

Laskar, J., Robutel, P., Joutel, F., Gastineau, M., Correia, A.C.M., Levrard, B., 2004. A long-term numerical solution for the insolation quantities of the Earth. A&A 428, 261—285.

Lézine, A.-M., Hély, C., Grenier, C., Braconnot, P., Krinner, G., 2011. Sahara and Sahel vulnerability to climate changes, lessons from Holocene hydrological data. Quat. Sci. Rev. 30, 3001—3012.

Lionello, P., Malanotte-Rizzoli, P., Boscolo, R., Alpert, P., Artale, V., Li, L., Luterbacher, J., May, W., Trigo, R., Tsimplis, M., Ulbrich, U., Xoplaki, E., 2006. The Mediterranean climate: an overview of the main characteristics and issues. In: Lionello, P., Malanotte-Rizzoli, P., Boscolo, R. (Eds.), Mediterranean Climate Variability. Elsevier, Amsterdam, The Netherlands, pp. 1—26.

Lisiecki, L., Raymo, M., 2005. A Pliocene-Pleistocene stack of 57 globally distributed benthic δ18O records. Paleoceanography 20, PA1003 doi:1010.1029/2004PA001071.

Lo Iacono, C., Savini, A., Basso, D., 2018. Cold-water carbonate bioconstructions. In: Micallef, A., Krastel, S., Savini, A. (Eds.), Submarine Geomorphology. Springer International Publishing, Cham, pp. 425—455.

Lo Iacono, C., Savini, A., Huvenne, V.A.I., Grācia, E., 2019. Habitat mapping of cold-water corals in the Mediterranean Sea. In: Orejas Saco del Valle, C., Jiménez, C. (Eds.), Mediterranean Cold-Water Corals: Past, Present and Future,

Springer Series: Coral Reefs of the World. Springer, pp. 157—171.

Lo Iacono, C., Gràcia, E., Ranero, C.R., Emelianov, M., Huvenne, V.A.I., Bartolomé, R., Booth-Rea, G., Prades, J., 2014. The West Melilla cold water coral mounds, Eastern Alboran Sea: morphological characterization and environmental context. Deep Sea Res. Part II 99, 316—326.

López Correa, M., Montagna, P., Joseph, N., Rüggeberg, A., Fietzke, J., Flögel, S., Dorschel, B., Goldstein, S.L., Wheeler, A., Freiwald, A., 2012. Preboreal onset of cold-water coral growth beyond the Arctic Circle revealed by coupled radio-carbon and U-series dating and neodymium isotopes. Quat. Sci. Rev. 34, 24—43.

Mangini, A., Godoy, J.M., Godoy, M.L., Kowsmann, R., Santos, G.M., Ruckelshausen, M., Schroeder-Ritzrau, A., Wacker, L., 2010. Deep sea corals off Brazil verify a poorly ventilated southern Pacific ocean during H2, H1 and the younger dryas. Earth Planet Sci. Lett. 293, 269—276.

Margirier, F., Testor, P., Heslop, E., Mallil, K., Bosse, A., Houpert, L., Mortier, L., Bouin, M.-N., Coppola, L., D'Ortenzio, F., Durrieu de Madron, X., Mourre, B., Prieur, L., Raimbault, P., Taillandier, V., 2020. Abrupt warming and salinisation of intermediate waters interplays with decline of deep convection in the Northwestern Mediterranean Sea. Sci. Rep. 10, 20923.

Margreth, S., Gennari, G., Rüggeberg, A., Comas, M.C., Pinheiro, L.M., Spezzaferri, S., 2011. Growth and demise of cold-water coral ecosystems on mud volcanoes in the West Alboran Sea: the messages from the planktonic and benthic forami-nifera. Mar. Geol. 282, 26—39.

Martínez-García, P., Soto, J.I., Comas, M., 2011. Recent structures in the Alboran Ridge and Yusuf fault zones based on swath bathymetry and sub-bottom profiling: evidence of active tectonics. Geo Mar. Lett. 31, 19—36.

Martorelli, E., Petroni, G., Chiocci, F.L., the Pantelleria Scientific, P., 2011. Contourites offshore Pantelleria Island (Sicily channel, Mediterranean sea): depositional, erosional and biogenic elements. Geo Mar. Lett. 31, 481—493.

Matos, L., Mienis, F., Wienberg, C., Frank, N., Kwiatkowski, C., Groeneveld, J., Thil, F., Abrantes, F., Cunha, M.R., Hebbeln, D., 2015. Interglacial occurrence of cold-water corals off Cape Lookout (NW Atlantic): first evidence of the Gulf Stream influence. Deep-Sea Res. Part I 105, 158—170.

McCulloch, M., Taviani, M., Montagna, P., López Correa, M., Remia, A., Mortimer, G., 2010. Proliferation and demise of deep-sea corals in the mediterranean during the younger dryas. Earth Planet Sci. Lett. 298, 143—152.

McGee, D., deMenocal, P.B., Winckler, G., Stuut, J.B.W., Bradtmiller, L.I., 2013. The magnitude, timing and abruptness of changes in North African dust deposition over the last 20,000yr. Earth Planet Sci. Lett. 371—372, 163—176.

Mienis, F., van Weering, T., de Haas, H., de Stigter, H., Huvenne, V., Wheeler, A., 2006. Carbonate mound development at the SW Rockall Trough margin based on high resolution TOBI and seismic recording. Mar. Geol. 233, 1—19.

Mienis, F., de Stigter, H.C., White, M., Duineveld, G., de Haas, H., van Weering, T.C.E., 2007. Hydrodynamic controls on cold-water coral growth and carbonate-mound development at the SW and SE Rockall Trough Margin, NE Atlantic Ocean. Deep Sea Res. Part I 54, 1655—1674.

Millot, C., 1999. Circulation in the western Mediterranean sea. J. Mar. Syst. 20, 423—442.

Millot, C., Taupier-Letage, I., 2005. Circulation in the Mediterranean sea. In: Saliot, A. (Ed.), The Mediterranean Sea. Springer, Berlin, Heidelberg, pp. 29—66.

Mohn, C., Rengstorf, A., White, M., Duineveld, G., Mienis, F., Soetaert, K., Grehan, A., 2014. Linking benthic hydrodynamics and cold-water coral occurrences: a high-resolution model study at three cold-water coral provinces in the NE Atlantic. Prog. Oceanogr. 122, 92—104.

Myers, P.G., Haines, K., Rohling, E.J., 1998. Modeling the paleocirculation of the mediterranean: the last glacial maximum and the Holocene with emphasis on the formation of sapropel S 1. Paleoceanography 13, 586—606.

Naumann, M.S., Orejas, C., Ferrier-Pagès, C., 2014. Species-specific physiological response by the cold-water corals Lophelia pertusa and Madrepora oculata to variations within their natural temperature range. Deep Sea Res. Part II 99, 36—41.

Orejas, C., Gori, A., Lo Iacono, C., Puig, P., Gili, J.M., Dale, M.R., 2009. Cold-water corals in the Cap de Creus canyon (north-western Mediterranean): spatial distribution, density and anthropogenic impact. Mar. Ecol. Prog. Ser. 397, 37—51.

Orejas, C., Wienberg, C., Titschack, J., Tamborrino, L., Freiwald, A., Hebbeln, D., 2021. Madrepora oculata forms large frameworks in hypoxic waters off Angola (SE Atlantic). Sci. Rep. 11, 15170.

Osborne, A.H., Marino, G., Vance, D., Rohling, E.J., 2010. Eastern Mediterranean surface water Nd during Eemian sapropel S5: monitoring northerly (mid-lati-tude) versus southerly (sub-tropical) freshwater contributions. Quat. Sci. Rev. 29, 2473—2483.

Parrilla, G., Kinder, T.H., Preller, R.H., 1986. Deep and intermediate mediterranean water in the western Alboran Sea. Deep-Sea Res. Part A Oceanogr. Res. Pap. 33, 55—88.

Past Interglacials Working Group of PAGES, 2016. Interglacials of the last 800,000 years. Rev. Geophys. 54, 162—219.

Pausata, F.S.R., Gaetani, M., Messori, G., Berg, A., Maia de Souza, D., Sage, R.F., deMenocal, P.B., 2020. The greening of the Sahara: past changes and future implications. One Earth 2, 235—250.

Pinardi, N., Masetti, E., 2000. Variability of the large scale general circulation of the Mediterranean Sea from observations and modelling: a review. Palaeogeogr. Palaeoclimatol. Palaeoecol. 158, 153—173.

Pirlet, H., Colin, C., Thierens, M., Latruwe, K., Van Rooij, D., Foubert, A., Frank, N., Blamart, D., Huvenne, V.A.I., Swennen, R., Vanhaecke, F., Henriet, J.-P., 2011. The importance of the terrigenous fraction within a cold-water coral mound: a case study. Mar. Geol. 282, 13—25.

Portilho-Ramos, R., Titschack, J., Wienberg, C., Siccha, M., Yokohama, Y., Hebbeln, D., 2022. Major environmental drivers determining life and death of cold-water corals through time. PLoS Biol. 20 (5), e3001628. https://doi.org/10.1371/journal.pbio.3001628.

Puig, P., Palanques, A., Guillén, J., El Khatab, M., 2004. Role of internal waves in the generation of nepheloid layers on the northwestern Alboran slope: implications for continental margin shaping. J. Geophys. Res.: Oceans 109.

Raddatz, J., Liebetrau, V., Rüggeberg, A., Foubert, A., Flögel, S., Nürnberg, D., Hissmann, K., Musiol, J., Goepfert, T.J., Eisenhauer, A., Dullo, W.-C., 2022. Living on the edge: environmental variability of a shallow late Holocene cold-water coral mound. Coral Reefs. https://doi.org/10.1007/s00338-022-02249-4.

Raddatz, J., Titschack, J., Frank, N., Freiwald, A., Conforti, A., Osborne, A., Skornitzke, S., Stiller, W., Rüggeberg, A., Voigt, S., Albuquerque, A.L.S., Vertino, A., Schröder-Ritzrau, A., Bahr, A., 2020. *Solenosmilia variabilis*-bearing cold-water coral mounds off Brazil. Coral Reefs 39, 69–83.

Railsback, L.B., Gibbard, P.L., Head, M.J., Voarintsoa, N.R.G., Toucanne, S., 2015. An optimized scheme of lettered marine isotope substages for the last 1.0 million years, and the climatostratigraphic nature of isotope stages and substages. Quat. Sci. Rev. 111, 94–106.

Remia, A., Taviani, M., 2005. Shallow-buried Pleistocene *madrepora*-dominated coral mounds on a muddy continental slope, Tuscan Archipelago, NE Tyrrhenian Sea. Facies 50, 419–425.

Revel, M., Ducassou, E., Grousset, F.E., Bernasconi, S.M., Migeon, S., Revillon, S., Mascle, J., Murat, A., Zaragosi, S., Bosch, D., 2010. 100,000 Years of African monsoon variability recorded in sediments of the Nile margin. Quat. Sci. Rev. 29, 1342–1362.

Roberts, J.M., Wheeler, A.J., Freiwald, A., 2006. Reefs of the deep: the biology and geology of cold-water coral ecosystems. Science 312, 543–547.

Roberts, J.M., Wheeler, A.J., Freiwald, A., Cairns, S.D., 2009. Cold-water Corals. In: The Biology and Geology of Deep-Sea Coral Habitats. Cambridge University Press.

Rodrigo-Gámiz, M., Martínez-Ruiz, F., Jiménez-Espejo, F.J., Gallego-Torres, D., Nieto-Moreno, V., Romero, O., Ariztegui, D., 2011. Impact of climate variability in the western Mediterranean during the last 20,000 years: oceanic and atmospheric responses. Quat. Sci. Rev. 30, 2018–2034.

Rohling, E.J., Marino, G., Grant, K.M., 2015. Mediterranean climate and oceanography, and the periodic development of anoxic events (sapropels). Earth Sci. Rev. 143, 62–97.

Rohling, E.J., Cane, T.R., Cooke, S., Sprovieri, M., Bouloubassi, I., Emeis, K.C., Schiebel, R., Kroon, D., Jorissen, F.J., Lorre, A., Kemp, A.E.S., 2002. African monsoon variability during the previous interglacial maximum. Earth Planet Sci. Lett. 202, 61–75.

Rossignol-Strick, M., 1985. Mediterranean Quaternary sapropels, an immediate response of the African monsoon to variation of insolation. Palaeogeogr. Palaeoclimatol. Palaeoecol. 49, 237–263.

Rüggeberg, A., Foubert, A., 2019. Cold-water corals and mud volcanoes: life on a dynamic substrate. In: Orejas Saco del Valle, C., Jiménez, C. (Eds.), Mediterranean Cold-Water Corals: Past, Present and Future, Springer Series: Coral Reefs of the World. Springer, pp. 265–269.

Sabatier, P., Nicolle, M., Piot, C., Colin, C., Debret, M., Swingedouw, D., Perrette, Y., Bellingery, M.-C., Chazeau, B., Develle, A.-L., Leblanc, M., Skonieczny, C., Copard, Y., Reyss, J.-L., Malet, E., Jouffroy-Bapicot, I., Maelle, K., Poulenard, J., Didier, J., Vannière, B., 2020. Past African dust inputs in the western Mediterranean area controlled by the complex interaction between the Intertropical Convergence Zone, the North Atlantic Oscillation, and total solar irradiance. Clim. Past 16, 283–298.

Sánchez-Guillamón, O., Rueda, J.L., Wienberg, C., Ercilla, G., Vázquez, J.T., Gómez-Ballesteros, M., Urra, J., Moya-Urbano, E., Estrada, F., Hebbeln, D., 2022. Morphosedimentary, structural and benthic characterization of carbonate mound fields on the upper continental slope of the northern Alboran sea (western mediterranean). Geosciences 12, 111.

Sandu, I., van Niekerk, A., Shepherd, T.G., Vosper, S.B., Zadra, A., Bacmeister, J., Beljaars, A., Brown, A.R., Dörnbrack, A., McFarlane, N., Pithan, F., Svensson, G., 2019. Impacts of orography on large-scale atmospheric circulation. Clim. Atmos. Sci. 2, 10.

Savini, A., Vertino, A., Marchese, F., Beuck, L., Freiwald, A., 2014. Mapping cold-water coral habitats at different scales within the northern Ionian Sea (central Mediterranean): an assessment of coral coverage and associated vulnerability. PLoS One 9, e87108.

Schroeder, K., Chiggiato, J., Josey, S.A., Borghini, M., Aracri, S., Sparnocchia, S., 2017. Rapid response to climate change in a marginal sea. Sci. Rep. 7, 4065.

Schroeder, K., Lafuente, J., Josey, S., Artale, V., Buongiorno Nardelli, B., Gacic, M., Gasparini, G.P., Herrmann, M., Lionello, P., Ludwig, W., Millot, C., Özsoy, E., Pisacane, G., Sánchez-Garrido, J., Sannino, G., Santoleri, R., Somot, S., Struglia, M., Stanev, E., Zodiatis, G., 2012. Circulation of the Mediterranean sea and its variability. In: Lionello, P. (Ed.), The Climate of the Mediterranean Region: from the Past to the Future. Elsevier, pp. 187–256.

Skliris, N., 2014. Past, present and future patterns of the thermohaline circulation and characteristic water masses of the Mediterranean sea. In: Goffredo, S., Dubinsky, Z. (Eds.), The Mediterranean Sea: its History and Present Challenges. Springer Netherlands, Dordrecht, pp. 29–48.

Smith, R.B., 1979. The influence of mountains on the atmosphere. In: Saltzman, B. (Ed.), Advances in Geophysics. Elsevier, pp. 87–230.

Stalder, C., Vertino, A., Rosso, A., Rüggeberg, A., Pirkenseer, C., Spangenberg, J.E., Spezzaferri, S., Camozzi, O., Rappo, S., Hajdas, I., 2015. Microfossils, a key to unravel cold-water carbonate mound evolution through time: evidence from the eastern Alboran Sea. PLoS One 10, e0140223.

Stalder, C., El Kateb, A., Vertino, A., Rüggeberg, A., Camozzi, O., Pirkenseer, C.M., Spangenberg, J.E., Hajdas, I., Van Rooij, D., Spezzaferri, S., 2018. Large-scale paleoceanographic variations in the western Mediterranean Sea during the last 34,000 years: from enhanced cold-water coral growth to declining mounds. Mar. Micropaleontol. 143, 46–62.

Struglia, M.V., Mariotti, A., Filograsso, A., 2004. river discharge into the Mediterranean sea: climatology and aspects of the observed variability. J. Clim. 17, 4740–4751.

Tamborrino, L., Wienberg, C., Titschack, J., Wintersteller, P., Mienis, F., Schröder-Ritzrau, A., Freiwald, A., Orejas, C., Dullo, W.-C., Haberkern, J., Hebbeln, D., 2019. Mid-Holocene extinction of cold-water corals on the Namibian shelf steered by the Benguela oxygen minimum zone. Geology 47, 1185–1188.

Taviani, M., Angeletti, L., Beuck, L., Campiani, E., Canese, S., Foglini, F., Freiwald, A., Montagna, P., Trincardi, F., 2016. Reprint of 'On and off the beaten track: megafaunal sessile life and Adriatic cascading processes. Mar. Geol. 375, 146–160.

Taviani, M., Angeletti, L., Canese, S., Cannas, R., Cardone, F., Cau, A., Cau, A.B., Follesa, M.C., Marchese, F., Montagna, P., Tessarolo, C., 2017. The "Sardinian cold-water coral province" in the context of the Mediterranean coral ecosystems. Deep Sea Res. Part II 145, 61–78.

Tesi, T., Asioli, A., Minisini, D., Maselli, V., Dalla Valle, G., Gamberi, F., Langone, L., Cattaneo, A., Montagna, P., Trincardi, F., 2017. Large-scale response of the Eastern Mediterranean thermohaline circulation to African monsoon intensification during sapropel S1 formation. Quat. Sci. Rev. 159, 139–154.

Tierney, J.E., Pausata, F.S.R., deMenocal, P.B., 2017. Rainfall regimes of the green Sahara. Sci. Adv. 3, e1601503.

Titschack, J., Thierens, M., Dorschel, B., Schulbert, C., Freiwald, A., Kano, A., Takashima, C., Kawagoe, N., Li, X., 2009. Carbonate budget of a cold-water coral mound (Challenger Mound, IODP Exp. 307). Mar. Geol. 259, 36–46.

Titschack, J., Baum, D., De Pol Holz, R., López Correa, M., Flögel, S., Hebbeln, D., Freiwald, A., 2015. Aggradation and carbonate accumulation of Holocene Norwegian cold-water coral reefs. Sedimentology 62, 1873–1898.

Titschack, J., Fink, H.G., Baum, D., Wienberg, C., Hebbeln, D., Freiwald, A., 2016. Mediterranean cold-water corals – an important regional carbonate factory? Depos. Rec. 2, 74–96.

Tjallingii, R., Claussen, M., Stuut, J.-B.W., Fohlmeister, J., Jahn, A., Bickert, T., Lamy, F., Rohl, U., 2008. Coherent high- and low-latitude control of the northwest African hydrological balance. Nat. Geosci. 1, 670–675.

Toucanne, S., Jouet, G., Ducassou, E., Bassetti, M.-A., Dennielou, B., Angue Minto'o, C.M., Lahmi, M., Touyet, N., Charlier, K., Lericolais, G., Mulder, T., 2012. A 130,000-year record of Levantine intermediate water flow variability in the Corsica trough, western Mediterranean. Quat. Sci. Rev. 33, 55–73.

van der Kaaden, A.-S., Mohn, C., Gerkema, T., Maier, S.R., de Froe, E., van de Koppel, J., Rietkerk, M., Soetaert, K., van Oevelen, D., 2021. Feedbacks between hydrodynamics and cold-water coral mound development. Deep Sea Res. Part I 178, 103641.

van der Land, C., Eisele, M., Mienis, F., de Haas, H., Hebbeln, D., Reijmer, J.J.G., van Weering, T.C.E., 2014. Carbonate mound development in contrasting settings on the Irish margin. Deep Sea Res. Part II 99, 297–306.

van Haren, H., 2014. Internal wave–zooplankton interactions in the Alboran Sea (W-Mediterranean). J. Plankton Res. 36, 1124–1134.

Van Rooij, D., De Mol, B., Huvenne, V.A.I., Ivanov, M., Henriet, J.P., 2003. Seismic evidence of current-controlled sedimentation in the Belgica mound province, upper Porcupine slope, southwest of Ireland. Mar. Geol. 195, 31–53.

Van Rooij D, Hebbeln D, Comas M, Vandorpe T, Delivet S, Nave S, Michel E, Lebreiro S, Terrinha P, Roque C, Anton L, Batista L, the MD 194 Shipboard Scientists (2017) MD 194/EUROFLEETS à bord du R/V Marion Dufresne. Cadix 10 juin 2013 - Lisbonne 20 juin 2013 Les Rapports de Campagnes à la Mer ISSN : vols. 1246–7375 ISBN: 2-910-180-81-6.

Vandorpe, T., Wienberg, C., Hebbeln, D., Van den Berghe, M., Gaide, S., Wintersteller, P., Van Rooij, D., 2017. Multiple generations of buried cold-water coral mounds since the early-middle Pleistocene transition in the Atlantic Moroccan coral province, southern Gulf of Cádiz. Palaeogeogr. Palaeoclimatol. Palaeoecol. 485, 293–304.

Vertino, A., Corselli, C., 2019. Did Quaternary climate fluctuations affect Mediterranean deep-sea coral communities? In: Orejas Saco del Valle, C., Jiménez, C. (Eds.), Mediterranean Cold-Water Corals: Past, Present and Future, Springer Series: Coral Reefs of the World. Springer, pp. 51–56.

Vertino, A., Taviani, M., Corselli, C., 2019. Spatio-temporal distribution of Mediterranean cold-water corals. In: Orejas Saco del Valle, C., Jiménez, C. (Eds.), Mediterranean Cold-Water Corals: Past, Present and Future, Springer Series: Coral Reefs of the World. Springer, pp. 67–83.

Vertino, A., Savini, A., Rosso, A., Di Geronimo, I., Mastrototaro, F., Sanfilippo, R., Gay, G., Etiope, G., 2010. Benthic habitat characterization and distribution from two representative sites of the deep-water SML Coral Province (Mediterranean). Deep Sea Res. II 57, 380–396.

Victorero, L., Blamart, D., Pons-Branchu, E., Mavrogordato, M.N., Huvenne, V.A.I., 2016. Reconstruction of the formation history of the Darwin Mounds, N Rockall Trough: how the dynamics of a sandy contourite affected cold-water coral growth. Mar. Geol. 378, 186–195.

Wang, H., Lo Iacono, C., Wienberg, C., Titschack, J., Hebbeln, D., 2019. Cold-water coral mounds in the southern Alboran Sea (western Mediterranean Sea): internal waves as an important driver for mound formation since the last

deglaciation. Mar. Geol. 412, 1–18.

Wang, H., Titschack, J., Wienberg, C., Korpanty, C., Hebbeln, D., 2021. The importance of ecological accommodation space and sediment supply for cold-water coral mound formation, a case study from the western Mediterranean Sea. Front. Mar. Sci. 8, 760909. https://doi.org/10.3389/fmars.2021.760909.

Wassenburg, J.A., Dietrich, S., Fietzke, J., Fohlmeister, J., Jochum, K.P., Scholz, D., Richter, D.K., Sabaoui, A., Spötl, C., Lohmann, G., Andreae Meinrat, O., Immenhauser, A., 2016. Reorganization of the north Atlantic oscillation during early Holocene deglaciation. Nat. Geosci. 9, 602–605.

Wefing, A.-M., Arps, J., Blaser, P., Wienberg, C., Hebbeln, D., Frank, N., 2017. High precision U-series dating of scleractinian cold-water corals using an automated chromatographic U and Th extraction. Chem. Geol. 475, 140–148.

Wheeler, A.J., Kozachenko, M., Henry, L.A., Foubert, A., de Haas, H., Huvenne, V.A.I., Masson, D.G., Olu, K., 2011. The Moira Mounds, small cold-water coral banks in the Porcupine Seabight, NE Atlantic: Part A—an early stage growth phase for future coral carbonate mounds? Mar. Geol. 282, 53–64.

White, M., Dorschel, B., 2010. The importance of the permanent thermocline to the cold water coral carbonate mound distribution in the NE Atlantic. Earth Planet Sci. Lett. 296, 395–402.

Wienberg, C., 2019. A deglacial cold-water coral boom in the Alboran Sea: from coral mounds and species dominance. In: Orejas Saco del Valle, C., Jiménez, C. (Eds.), Mediterranean Cold-Water Corals: Past, Present and Future, Springer Series: Coral Reefs of the World. Springer, pp. 57–60.

Wienberg, C., Titschack, J., 2017. Framework-forming scleractinian cold-water corals through space and time: a late Quaternary North Atlantic perspective. In: Rossi, S., Bramanti, L., Gori, A., Orejas Saco del Valle, C. (Eds.), Marine Animal Forests: the Ecology of Benthic Biodiversity Hotspots. Springer, Cham, pp. 699–732.

Wienberg, C., Frank, N., Mertens, K.N., Stuut, J.-B., Marchant, M., Fietzke, J., Mienis, F., Hebbeln, D., 2010. Glacial cold-water coral growth in the Gulf of Cadiz: implications of increased palaeo-productivity. Earth Planet Sci. Lett. 298, 405–416.

Wienberg, C., Titschack, J., Frank, N., De Pol-Holz, R., Fietzke, J., Eisele, M., Kremer, A., Hebbeln, D., 2020. Deglacial upslope shift of NE Atlantic intermediate waters controlled slope erosion and cold-water coral mound formation (Porcupine Seabight, Irish margin). Quat. Sci. Rev. 237, 106310.

Wienberg, C., Titschack, J., Freiwald, A., Frank, N., Lundälv, T., Taviani, M., Beuck, L., Schröder-Ritzrau, A., Krengel, T., Hebbeln, D., 2018. The giant Mauritanian cold-water coral mound province: oxygen control on coral mound formation. Quat. Sci. Rev. 185, 135–152.

Würtz, M., Rovere, M., 2015. Atlas of the Mediterranean Seamounts and Seamount-like Structures. IUCN, Gland, Switzerland and Málaga, Spain.

Ziegler, M., Tuenter, E., Lourens, L.J., 2010. The precession phase of the boreal summer monsoon as viewed from the eastern Mediterranean (ODP Site 968). Quat. Sci. Rev. 29, 1481–1490.